

UNIVERSIDADE FEDERAL DE UBERLÂNDIA
INSTITUTO DE CIÊNCIAS BIOMÉDICAS
PROGRAMA DE PÓS-GRADUAÇÃO EM IMUNOLOGIA E PARASITOLOGIA
APLICADAS

MARIANA ARAÚJO COSTA

SELEÇÃO E CARACTERIZAÇÃO DE BIOMARCADORES POR PHAGE DISPLAY E
DESENVOLVIMENTO DE PLATAFORMAS IMUZOENZIMÁTICA E BIOFOTÔNICA
PARA DETECÇÃO DA DOENÇA HEPATITE DELTA

UBERLÂNDIA - MG

2023

MARIANA ARAÚJO COSTA

SELEÇÃO E CARACTERIZAÇÃO DE BIOMARCADORES POR PHAGE DISPLAY E
DESENVOLVIMENTO DE PLATAFORMAS IMUZOENZIMÁTICA E BIOFOTÔNICA
PARA DETECÇÃO DA DOENÇA HEPATITE DELTA

Tese de Doutorado apresentada ao Programa
de Pós-Graduação em Imunologia e
Parasitologia Aplicadas como requisito
parcial para obtenção do título de Doutor (a).

Área de concentração: Imunologia e
Parasitologia Aplicadas

Orientador: Prof. Dr. Robinson Sabino da
Silva

Coorientadora: Profa. Dra. Fabiana de
Almeida Araújo Santos

UBERLÂNDIA - MG

2023

Ficha Catalográfica Online do Sistema de Bibliotecas da UFU
com dados informados pelo(a) próprio(a) autor(a).

C837
2023

Costa, Mariana Araújo, 1992-

Seleção e caracterização de biomarcadores por phage display e desenvolvimento de plataformas imunoenzimática e biofotônica para detecção da doença hepatite delta [recurso eletrônico] / Mariana Araújo Costa. - 2023.

Orientador: Robinson Sabino da Silva.

Coorientadora: Fabiana de Almeida Araújo Santos.

Tese (Doutorado) - Universidade Federal de Uberlândia,
Pós-graduação em Imunologia e Parasitologia Aplicadas.

Modo de acesso: Internet.

Disponível em: <http://doi.org/10.14393/ufu.te.2023.596>

Inclui bibliografia.

Inclui ilustrações.

1. Imunologia. I. Silva, Robinson Sabino da, 1981-,
(Orient.). II. Santos, Fabiana de Almeida Araújo, 1983-,
(Coorient.). III. Universidade Federal de Uberlândia.
Pós-graduação em Imunologia e Parasitologia Aplicadas.
IV. Título.

CDU: 612.017

Bibliotecários responsáveis pela estrutura de acordo com o AACR2:

Gizele Cristine Nunes do Couto - CRB6/2091
Nelson Marcos Ferreira - CRB6/3074



ATA DE DEFESA - PÓS-GRADUAÇÃO

Programa de Pós-Graduação em	Imunologia e Parasitologia Aplicadas				
Defesa de:	Tese de Doutorado nº 158				
Data:	doze de dezembro de dois mil e vinte e três	Hora de início:	13:30	Hora de encerramento:	17:35
Matrícula do Discente:	11923IPA014				
Nome do Discente:	Mariana Araújo Costa				
Título do Trabalho:	Seleção de inovadoras moléculas bioativas via phage display e desenvolvimento de plataformas imunoenzimática e biofotônica para detecção de hepatite delta				
Área de concentração:	Imunologia e Parasitologia Aplicadas				
Linha de pesquisa:	Biologia das interações entre patógenos e seus hospedeiros				
Projeto de Pesquisa de vinculação:	Rede de pesquisa em doenças infecciosas humanas e animais no estado de minas gerais				

Em 12 de dezembro de 2023, às 13:30h, reuniu-se por vídeo conferência, a Banca Examinadora, designada pelo Colegiado do Programa de Pós-graduação em Imunologia e Parasitologia Aplicadas, assim composta pelos membros titulares: Robinson Sabino da Silva - ICBIM/UFU (Presidente) orientador da candidata; Emilia Rezende Vaz - IBTEC/UFU; Diego Pandeló José - UFTM - Iturama; Livia Melo Villar - LAHEP/IOC; Marcelo Simão Ferreira - FAMED/UFU.

Iniciando os trabalhos o presidente da mesa, Prof. Dr. Robinson Sabino da Silva, apresentou a Comissão Examinadora e a candidata, agradeceu a presença do público, e concedeu ao Discente a palavra para a exposição do seu trabalho. A duração da apresentação, o tempo de arguição e resposta foram conforme as normas do Programa.

A seguir o senhor(a) presidente concedeu a palavra, pela ordem sucessivamente, aos(às) examinadores(as), que passaram a arguir o(a) candidato(a). Ultimada a arguição, que se desenvolveu dentro dos termos regimentais, a Banca, em sessão secreta, atribuiu o resultado final, considerando o(a) candidato(a):

APROVADO

Esta defesa faz parte dos requisitos necessários à obtenção do título de Doutor.

O competente diploma será expedido após cumprimento dos demais requisitos, conforme as normas do Programa, a legislação pertinente e a regulamentação interna da UFU.

Nada mais havendo a tratar foram encerrados os trabalhos. Foi lavrada a presente ata que após lida e achada conforme foi assinada pela Banca Examinadora.



Documento assinado eletronicamente por **Robinson Sabino da Silva, Professor(a) do Magistério Superior**, em 12/12/2023, às 17:37, conforme horário oficial de Brasília, com fundamento no art. 6º, § 1º, do [Decreto nº 8.539, de 8 de outubro de 2015](#).



Documento assinado eletronicamente por **Emília Rezende Vaz, Usuário Externo**, em 12/12/2023, às 17:39, conforme horário oficial de Brasília, com fundamento no art. 6º, § 1º, do [Decreto nº 8.539, de 8 de outubro de 2015](#).



Documento assinado eletronicamente por **Livia Melo Villar, Usuário Externo**, em 12/12/2023, às 17:39, conforme horário oficial de Brasília, com fundamento no art. 6º, § 1º, do [Decreto nº 8.539, de 8 de outubro de 2015](#).



Documento assinado eletronicamente por **Diego Pandeló José, Usuário Externo**, em 12/12/2023, às 17:42, conforme horário oficial de Brasília, com fundamento no art. 6º, § 1º, do [Decreto nº 8.539, de 8 de outubro de 2015](#).



Documento assinado eletronicamente por **Marcelo Simão Ferreira, Professor(a) do Magistério Superior**, em 19/12/2023, às 09:45, conforme horário oficial de Brasília, com fundamento no art. 6º, § 1º, do [Decreto nº 8.539, de 8 de outubro de 2015](#).



A autenticidade deste documento pode ser conferida no site https://www.sei.ufu.br/sei/controlador_externo.php?acao=documento_conferir&id_orgao_acesso_externo=0, informando o código verificador **5014496** e o código CRC **EB365241**.

AGRADECIMENTO

À minha mãe que me acompanhou em todas as etapas e que me incentivou desde o início deste projeto.

Ao meu pai (*in memoriam*) que foi de grande importância em minha carreira acadêmica.

Ao LACEN/AC, em especial a Taynã, minha gerente que me incentivou e ajudou em todo o processo para conseguir executar o projeto em Uberlândia (MG). À Janaina que me ajudou com seu vasto conhecimento técnico dos exames executados no LACEN. Aos meus amigos de bancada do COVID: Rafa, Uiu, Leandro, Camilo, Ruth, Suenia e Zena, sempre pude contar com vocês. Ao Fernando Abreu, Cristiano Souza, Aglanair, Jaqueline Bestene e Mira que me apoiaram para que a execução dos experimentos deste trabalho fosse realizada em Uberlândia. Ao professor Miguel Bortolini que me apoiou para o ingresso no programa de pós-graduação do PIPPA/UFU.

À Secretaria de Saúde do Acre pela compressão e apoio para que eu pudesse realizar os experimentos presencialmente em Uberlândia, em especial a secretária de saúde Ana Paula Mariano.

Ao setor de sorologia do LACEN/AC em especial a Greice, Carmem e Francilene pela ajuda na etapa de armazenamento e separação das amostras.

Aos colaboradores deste projeto Merieux, em especial a Ruth, Daniel, Fellype e Yan.

À Fabys, minha coorientadora, muito obrigada por ter me “adotado” no laboratório Nanos. Sempre será um grande exemplo de pesquisadora e ser humano. Muito obrigada pelas discussões e orientações. Vou sentir muita falta da minha amiga de bancada.

Aos meus amigos e colegas do laboratório Ray, Marco, Douglas, “Banner”, Mayla, Iara, Sabrina, Emília, Mário, Lucas, Abel, Hebréia, Natieli, Ester, Tafa, Luciana e Natassia que contribuíram para minha formação, sempre foram muito solícitos quando eu precisava de ajuda.

Ao meu orientador Robinson, muito obrigada pela oportunidade, pelos conselhos, paciência e solicitude. O tempo que pude conviver em Uberlândia foi muito proveitoso e pude conviver com um grande pesquisador e ser humano.

À FIOCRUZ Rondônia, Ana, Adryan, Tarcio, Carol, Melquias, Jackson e Dra. Deusilene por me receberem e por toda a contribuição ao trabalho.

À CAPES, CNPq e FAPEMIG, que pelo auxílio financeiro através do INCT TeraNano, permitiu a execução desse projeto.

Ao meu primeiro orientador deste projeto Luiz Ricardo Goulart Filho (*in memoriam*) pela confiança e incentivo de iniciar este trabalho. Infelizmente pela COVID-19 não pude conhecê-lo pessoalmente.

RESUMO

O vírus da hepatite Delta (HDV) é um vírus peculiar, comumente classificado como vírus satélite do vírus da hepatite B (HBV) devido a dependência para completar seu ciclo de replicação. No Brasil, entre os anos de 2000 e 2021, foram notificados um total de 4.259 casos de hepatite Delta, sendo a maioria (73,7%) dos casos notificados da região Norte. A infecção pelo HDV é a forma mais grave entre as hepatites virais apresentando maior risco de desenvolvimento de cirrose e de progressão rápida para carcinoma hepatocelular em comparação à monoinfecção pelo HBV. Portanto o exame diagnóstico do HDV é recomendado para todos os pacientes com infecção crônica pelo HBV. A presente tese é composta por dois capítulos referentes ao desenvolvimento de plataformas para o diagnóstico do HDV. No primeiro capítulo, é apresentada a aplicação da Espectroscopia de Infravermelho com Transformada de Fourier com Refletância Total Atenuada (ATR-FTIR) suportada por algoritmos de inteligência artificial como ferramenta para triagem da hepatite Delta. Em uma coorte com 359 pacientes, esta plataforma biofotônica utilizando 10 µL de soro permitiu a discriminação rápida, portátil, sustentável, sem utilização de reagentes de pacientes com sorologia positiva para hepatite Delta em comparação à sujeitos controles negativos para hepatite B e hepatite C com sorologia negativa para anticorpos contra HBV (anti-HBs), sujeitos controles negativos para hepatite B e hepatite C com sorologia positiva anti-HBs e pacientes com hepatite B apresentando, respectivamente, acurácia de 80%, 82% e 74% suportada por algoritmos de Suporte de Vetores de Máquinas (SVM). No segundo capítulo, está descrito a utilização da tecnologia de *Phage Display* para a seleção de moléculas miméticas ao HDV. O produto desta seleção permitiu a construção de uma proteína recombinante nomeada HDAgProt, que quando aplicada em plataforma imunoenzimática para detectar anti-HDV em comparação a pacientes com hepatite B apresentou sensibilidade de 74,71%, especificidade de 97,85%; e área sob a curva (AUC) de 0.8906. A análise específica de pacientes com infecção ativa de HDV baseada em teste por RT-qPCR apresentou incremento na taxa de detecção com sensibilidade de 88,00%, especificidade de 98,92%, e AUC de 0.9411 em comparação a pacientes com hepatite B. O conjunto dos dados desta tese de doutorado indica que a plataforma biofotônica sustentável sem uso de reagentes suportada por algoritmos de inteligência artificial e a seleção de moléculas por tecnologia *Phage display* inserida em testes imunoenzimáticos apresentam grande potencial para detecção de hepatite delta (HDV).

Palavras chave: HDV; diagnóstico; *Phage Display*; imunoenzimático; sustentabilidade.

ABSTRACT

Hepatitis Delta virus (HDV) is a peculiar virus, commonly classified as a satellite virus agent of hepatitis B virus (HBV) due to its dependency to complete the replication cycle. In Brazil, between 2000 and 2021, a total of 4,259 cases of Delta hepatitis were reported, with the majority (73.7%) of cases reported from the North region. HDV infection is the most serious form of viral hepatitis, presenting a higher risk of developing cirrhosis and rapid progression to hepatocellular carcinoma compared to HBV mono-infection. Therefore, HDV diagnostic testing is recommended for all patients with chronic HBV infection. This thesis is composed of two chapters relating to the development of platforms for the diagnosis of HDV. In the first chapter, the application of Fourier Transform Infrared Spectroscopy with Attenuated Total Reflectance (ATR-FTIR) supported by artificial intelligence algorithms as a tool for screening hepatitis Delta is presented. In a cohort of 359 patients, this biophotonic platform using 10 μ L of serum allowed rapid, portable, sustainable discrimination, without the use of reagents, of patients with positive serology for hepatitis Delta in comparison to control subjects negative for hepatitis B and hepatitis C with negative serology for antibodies against HBV (anti-HBs), control subjects negative for hepatitis B and hepatitis C with positive anti-HBs serology, and patients with hepatitis B presenting, respectively, with an accuracy of 80%, 82%, and 74% supported by Support algorithms of Machine Vectors (SVM). The second chapter describes the use of Phage Display technology for the selection of HDV-mimetic molecules. The product of this selection allowed the construction of a recombinant protein called HDAgProt, which when applied on an immunoenzymatic platform to detect anti-HDV in comparison to patients with hepatitis B presented a sensitivity of 74.71%, specificity of 97.85%; an area under the curve (AUC) of 0.8906. The specific analysis of patients with active HDV infection based on RT-qPCR testing showed an increase in the detection rate with a sensitivity of 88.00%, specificity of 98.92%, and AUC of 0.9411 compared to patients with hepatitis B. The set of data from this doctoral thesis indicates that the sustainable biophotonic platform without the use of reagents supported by artificial intelligence algorithms and the selection of molecules using Phage display technology inserted in immunoenzymatic tests have great potential for detecting hepatitis delta (HDV).

Keywords: HDV; diagnostics; *Phage Display*; immunoenzymatic; ATR-FTIR; sustainability.

LISTA DE ABREVIATURA

ALT - Alanina aminotransferase

Anti-HBs - Anticorpo contra o antígeno de superfície do vírus da hepatite B

Anti-HDAg - Anticorpo contra o antígeno da hepatite Delta

AST - Aspartato aminotransferase

ATR-FTIR - Espectroscopia no infravermelho por transformada de Fourier com reflectância total atenuada

DNA - Ácido desoxirribonucleico

Fiocruz/RO - Fundação Oswaldo Cruz Rondônia

HBsAg - Antígeno de superfície do vírus da hepatite B

HBV - Vírus da hepatite B

HDAg - Antígeno do vírus da hepatite Delta

HDV - Vírus da hepatite Delta

ICTV - Comitê Internacional de Taxonomia

IgG - Imunoglobulina G

IgM - Imunoglobulina M

LAMP - Amplificação isotérmica mediada em alça

L-HBsAg - Antígeno de superfície do vírus da hepatite B- *Large*

L-HDAg - Antígeno do vírus da hepatite Delta- *Large*

M-HBsAg - Antígeno de superfície da hepatite B- *Medium*

NLS - Sítio de localização nuclear

NTCP - Polipeptídio cotransportador Taurocolato de sódio

OMS - Organização Mundial de Saúde

ORF - Fase de leitura aberta (*open reading frame*)

PPIPA/UFU - Programa de Pós-graduação em Imunologia e Parasitologia Aplicadas

RNA - Ácido ribonucleico

RNP - Ribonucleoproteína

RTqPCR - Reação em cadeia da polimerase via transcriptase reversa quantitativa

SalivaNano - Grupo de Inovação em Diagnóstico Salivar e Nanobiotecnologia

S-HBsAg - Antígeno de superfície do vírus da hepatite B- *Small*

S-HDAg - Antígeno do vírus da hepatite Delta- *Small*

UESB - Universidade Estadual do Sudoeste da Bahia

SUMÁRIO

APRESENTAÇÃO	12
1 FUNDAMENTAÇÃO TEÓRICA.....	13
1.1 Histórico	13
1.2 Agente etiológico e morfologia.....	13
1.3 Ciclo de multiplicação viral.....	15
1.4 Epidemiologia no mundo e no Brasil.....	16
1.5 Transmissão e profilaxia da hepatite Delta	18
1.6 Doença e evolução clínica da hepatite Delta	18
1.7 Diagnóstico.....	20
1.8 Espectroscopia no Infravermelho por Transformada de Fourier com Reflectância Total Atenuada (ATR-FTIR)	21
1.9 <i>Phage Display</i>	24
2 OBJETIVO	26
2.1 Objetivo geral.....	26
2.2 Objetivos específicos	26
CAPÍTULO I	27
CAPÍTULO II.....	46
3 CONCLUSÕES	74
REFERÊNCIAS	75

APRESENTAÇÃO

A presente tese de Doutorado foi originalmente idealizada pela equipe do Laboratório de Saúde Pública do Acre juntamente com o professor Dr. Luiz Ricardo Goulart Filho (*in memoriam*). Posteriormente, a pesquisa foi agregada ao Grupo de Inovação em Diagnóstico Salivar e Nanobiotecnologia (SalivaNano), contando com a colaboração do Centro de Infectologia Charles Merieux & Laboratório Rodolphe Merieux, Fundação Oswaldo Cruz Rondônia (FIOCRUZ/RO), Faculdade de Computação (FACOM/UFU) e o Laboratório de Bioinformática e Química Computacional (UESB). Os experimentos foram realizados na sua totalidade no Laboratório de Nanobiotecnologia Prof. Dr. Luiz Ricardo Goulart Filho – IBTEC/UFU.

A estrutura deste trabalho seguiu as normas do Programa de Pós-graduação em Imunologia e Parasitologia Aplicadas (PPIPA/UFU), apresentando as seguintes seções.

- Fundamentação teórica – Revisão de literatura sobre o vírus da hepatite D, ATR-FTIR e *Phage Display*.
- Capítulo I – “*A combined high-throughput, portable and sustainable ATR-FTIR platform for hepatitis D detection in serum of a large patient cohort from Brazilian Amazon*”. Artigo para ser submetido ao periódico “Scientific Reports” com fator de impacto 4.997, cujo os critérios para submissão estão disponíveis em: <https://www.nature.com/srep/author-instructions/submission-guidelines>.
- Capítulo II – “*Novel Epitope-Based Diagnostic Probes Selected by Phage Display for Serological Detection of HDV*”. Artigo para ser submetido ao periódico “Scientific Reports” com fator de impacto 4.997, cujo os critérios para submissão estão disponíveis em: <https://www.nature.com/srep/author-instructions/submission-guidelines>.
- Considerações finais. Principais contribuições dos resultados desta tese.

1 FUNDAMENTAÇÃO TEÓRICA

1.1 Histórico

Um importante marco para a descoberta do vírus da hepatite Delta (HDV) ocorreu na Itália em 1977. Foi demonstrado a detecção de um antígeno Delta na análise das biópsias hepáticas em amostras de pacientes com sorologia positiva para o antígeno de superfície do vírus da hepatite B (HBsAg). Adicionalmente, nestes pacientes foi observado a presença de anticorpos contra o antígeno Delta em amostras de soro. O sistema antígeno/anticorpo Delta recém-descoberto foi identificado em pacientes que têm hepatite B crônica, especialmente entre aqueles com lesões hepáticas mais severas (Rizzetto *et al.*, 1977).

Em 1980, baseado em modelo animal de chimpanzés expostos ao soro de pacientes com sorologia positiva para HBsAg e Delta, o antígeno Delta foi associado ao vírus da hepatite B (HBV). Foi demonstrado que chimpanzés com sorologia positiva para o anticorpo contra o antígeno de superfície do vírus da hepatite B (anti-HBs) não apresentavam a detecção do antígeno Delta, no entanto, nos chimpanzés portadores crônicos de hepatite B ocorreu aumento significativo de antígeno Delta intra-hepático. Inicialmente, foi sugerido que o antígeno Delta seria um novo marcador de um patógeno ainda desconhecido, uma variante do vírus da hepatite B (HBV) ou um novo agente viral que necessitaria do auxílio do HBV para a infecção (Botelho-Souza *et al.*, 2017; Rizzetto, *et al.*, 1980a).

Posteriormente, novas pesquisas demonstraram que o antígeno Delta era uma proteína de um novo vírus, distinto do vírus da hepatite B. Foi descrita uma associação entre o antígeno delta, HBsAg e um pequeno RNA em soro de chimpanzés infectados com Delta, fornecendo evidências sobre a existência de um novo vírus de hepatite (Rizzetto, M. *et al.*, 1980b). Em 1986, foi apresentado pela primeira vez o genoma do vírus da hepatite Delta, sendo identificado o primeiro vírus que possui genoma de RNA circular de fita simples capaz de infectar animais (Wang *et al.*, 1986).

1.2 Agente etiológico e morfologia

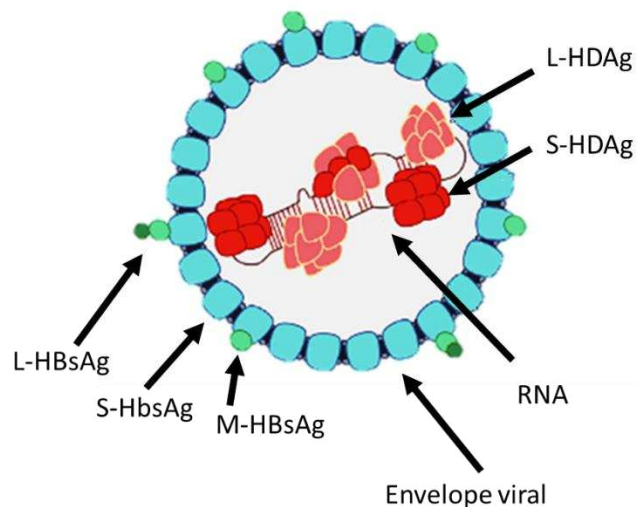
O HDV, segundo o Comitê Internacional de Taxonomia (ICTV), é pertencente ao reino *Ribozyviria*, família *Kolmioviridae* e gênero *Deltavirus*. Este vírus é classificado frequentemente como vírus satélite do HBV ou agente sub-viral, devido à sua incapacidade de

infecção na ausência do HBV, pois o HDV necessita de proteínas do HBV para completar seu ciclo de multiplicação (Botelho-Souza *et al.*, 2017; Cunha; Tavanetz; Gudima, 2015; Perez-Vargas *et al.*, 2019).

O HDV é caracterizado por apresentar o tamanho de 35-37nm, seu formato é esférico, circundado por um envelope que contém três proteínas provenientes do vírus da hepatite B (S-HBsAg, M-HBsAg e L-HBsAg) (Mentha *et al.*, 2019). As três proteínas compartilham a região C-terminal, a proteína S-HBsAg contém somente o domínio S, enquanto a M-HBsAg tem um domínio hidrofílico N-terminal PreS2 e a proteína L-HBsAg possui um domínio adicional, denominado de PreS1 conforme (Figura 1) (Da; Heller; Koh, 2019; Mentha *et al.*, 2019).

O genoma do HDV é circular, pequeno, com cerca de 1,7Kb, apresenta RNA de fita simples com polaridade negativa, apresentando um significativo pareamento interno (cerca de 70% de seus nucleotídeos pareados), o que permite seu dobramento e faz com que seu formato estrutural seja semelhante a um bastão parcialmente de fita dupla que é incapaz de codificar suas proteínas isoladamente (Pierre *et al.*, 2022). O genoma do HDV codifica uma proteína a HDaAg, que apresenta duas formas S-HDaAg (“S” *small*: pequena) e L-HDaAg (“L” *large*: grande). As duas isoformas são idênticas, exceto que o L-HDaAg tem uma sequência adicional de 19 aminoácidos no C-terminal (Asselah; Rizzetto, 2023; Cunha; Tavanetz; Gudima, 2015; Da; Heller; Koh, 2019; Sureau; Negro, 2016). Ambas as isoformas encontram-se complexadas ao RNA viral constituindo a Ribonucleoproteína (RNP) (Cunha; Tavanetz; Gudima, 2015; Da; Heller; Koh, 2019; Mentha *et al.*, 2019).

Figura 1- Representação da partícula do vírus da hepatite Delta.



O HDV está envolto pelo antígeno de superfície do HBV. Na porção central, o HDaAg (antígeno da hepatite Delta) na forma S-HDaAg (“S” *small*: pequena) e L-HDaAg (“L” *large*: grande) e no centro o genoma do HDV.
Fonte: Adaptado de (Lucifora; Delphin, 2020).

1.3 Ciclo de multiplicação viral

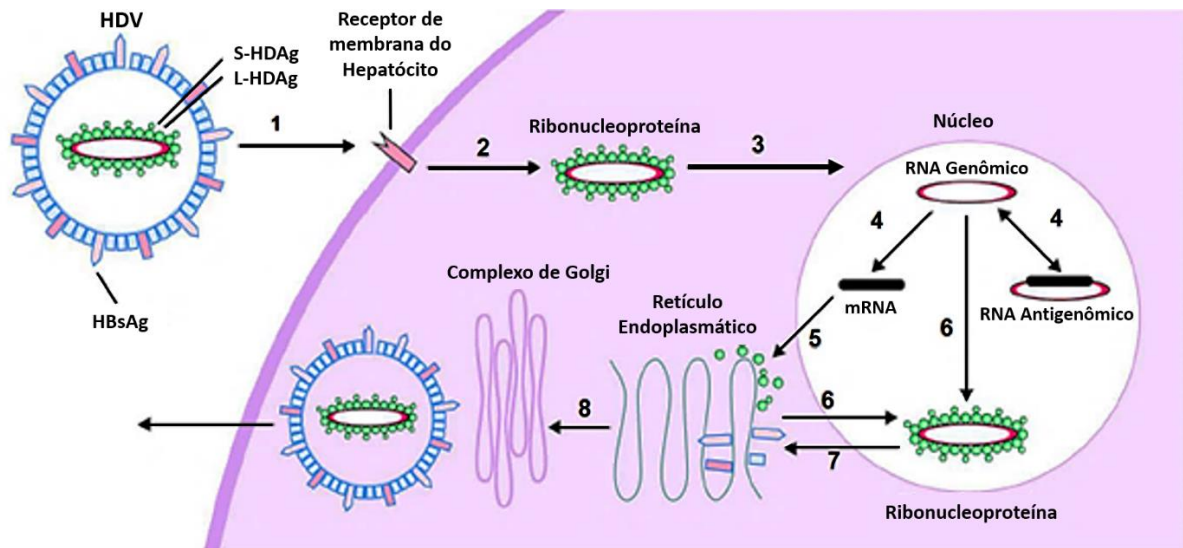
A primeira etapa do ciclo de multiplicação é a adsorção, na qual o vírus interage com receptores celulares, no caso do HDV, ocorre uma ligação de baixa especificidade e afinidade com proteoglicanos de heparan sulfato presentes na membrana plasmática de células hospedeiras. Esta ligação estabiliza o vírus na superfície celular promovendo uma ligação de alta afinidade da proteína L-HBsAg com receptor Polipeptídeo cotransportador Taurocolato de sódio (NTCP) (Botelho-Souza *et al.*, 2017; Heuschkel; Baumert; Verrier, 2021; Pierre *et al.*, 2022, 2022; Yan *et al.*, 2012). Após a adsorção ocorre a penetração do HDV via endocitose. (Figura 2) (Herrscher; Roingeard; Blanchard, 2020; Heuschkel; Baumert; Verrier, 2021; Asselah; Rizzetto, 2023).

Durante a etapa da penetração, ocorre o desnudamento da partícula viral no citoplasma liberando a ribonuclueproteína (RNP) que é transportada até o núcleo da célula, através do sítio de localização nuclear (NLS) presente na HDAG que interage com importinas celulares (Chou *et al.*, 1998). No núcleo da célula, a replicação viral é mediada pela RNA polimerase II do hospedeiro (Greco-Stewart *et al.*, 2007; Greco-Stewart; Schissel; Pelchat, 2009). Há evidências que a RNA polimerase tipo I e III também se ligam ao RNA viral, sendo a RNA polimerase do tipo I envolvida na transcrição do RNA antígenômico (RNA complementar ao do vírus denominado RNA genômico) (Greco-Stewart; Schissel; Pelchat, 2009).

O mecanismo de replicação é denominado círculo-rolante (Asselah; Rizzetto, 2023). Este mecanismo é iniciado com a ação da RNA polimerase II com auxílio da proteína viral S-HDAG, que irá gerar o RNA antígenômico a partir da fita de RNA negativa do HDV. O RNA antígenômico servirá como molde para síntese de fitas de RNA genômico. A partir do RNA genômico também é sintetizado um pequeno RNA antígenômico que contém a ORF que codifica as duas formas da proteína HDAG (antígeno Delta) (Da; Heller; Koh, 2019; Koh; Da; Glenn, 2019). A síntese das proteínas L-HDAG e a S-HDAG se deve a tradução de dois RNA mensageiros distintos produzidos, que ocorre devido ação da enzima humana adenosina desaminase, que pode realizar eventos catalíticos e edição do código de parada no RNA antígenômico responsável pela tradução da S-HDAG. Isto pode acarretar a extensão da região de leitura permitindo também a síntese da L-HDAG. Subsequentemente, S-HDAG e L-HDAG são traduzidas no retículo endoplasmático (Da; Heller; Koh, 2019; Koh; Da; Glenn, 2019; Pierre *et al.*, 2022) e enviadas ao núcleo para associação ao RNA genômico para formar as RNPs que serão exportadas para o citoplasma, com subsequente interação com as proteínas do envelope do HBV através do L-HDAG no retículo endoplasmático. A interação da proteína L-

HDAg com a proteína do HBV é possível devido a farnesilação da L-HDAg. Após a interação das proteínas do envelope do HBV, a ribonucleoproteína do HDV, o vírus será liberado pela rede trans-Golgi para ambiente extra-celular, onde poderá infectar novos hepatócitos (Botelho-Souza *et al.*, 2017; Da; Heller; Koh, 2019).

Figura 2- Representação do ciclo de multiplicação do HDV.



(1) A primeira etapa é a adsorção do vírion ao receptor do hepatócito. (2) Subsequentemente ocorre a penetração e desnudamento do HDV no citoplasma celular. (3) A ribonucleoproteína do HDV é direcionada ao núcleo da célula. (4) Na região nuclear o RNA genômico dá origem ao RNA antigenômico e mRNA. (5) O mRNA é transportado para o citoplasma, para tradução da proteína viral HDAg no retículo endoplasmático. (6) As proteínas recém-sintetizadas retornam ao núcleo e se associam ao RNA genômico, formando novas ribonucleoproteínas. (7) Estas ribonucleoproteínas são transportadas para o citoplasma onde se associam às proteínas do envelope do HBV no retículo endoplasmático. (8) As partículas virais são transportadas ao Complexo de Golgi para finalização do empacotamento e, subsequente, liberação do vírus para infectar novas células.

Fonte: Adaptado de (Brasil, 2018; Hughes; Wedemeyer; Harrison, 2011).

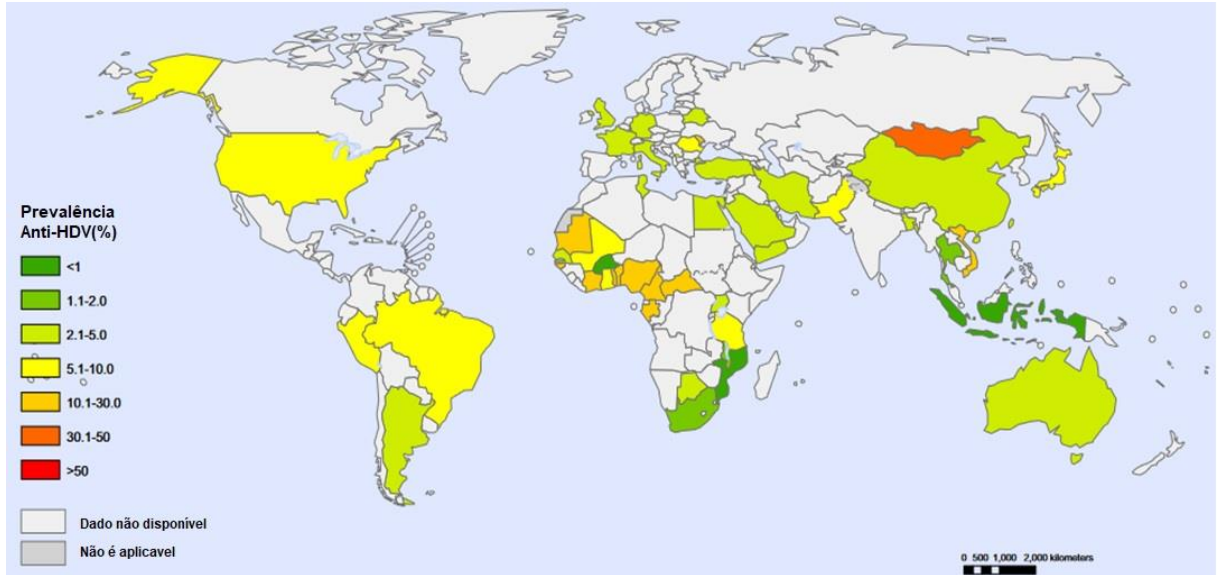
1.4 Epidemiologia no mundo e no Brasil

Os dados de prevalência mostram que a hepatite Delta é uma doença amplamente distribuída no mundo, estima-se que a prevalência de HDV é de aproximadamente 12 milhões de pessoas, ou seja, 4,5% dos portadores crônicos de hepatite B também são positivos para hepatite Delta (Stockdale *et al.*, 2020). Os países de maior prevalência são os subdesenvolvidos, sendo a Mongólia o país de maior prevalência de Delta, com uma taxa de 36,9% em indivíduos com sorologia positiva para HBsAg (Rizzetto, 2015; Stockdale *et al.*, 2020) (Figura 3).

No Brasil, entre os anos de 2000 e 2022, foram notificados um total de 4.393 casos de hepatite Delta, sendo que a maioria dos casos notificados é da região Norte, totalizando um

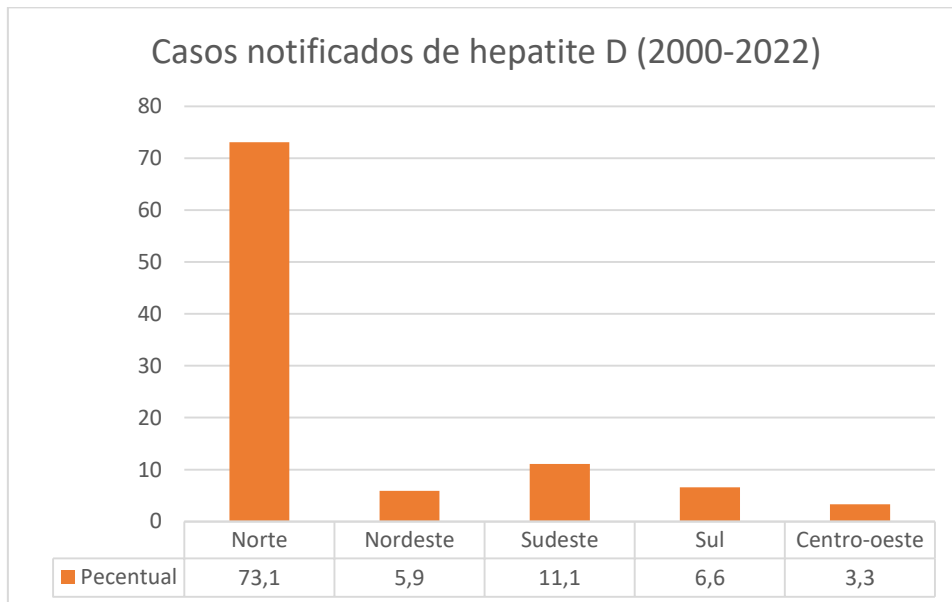
percentual de 73,1% dos casos. A região Sudeste apresenta 11,1% dos casos, a região Sul apresenta 6,6% dos casos, e as regiões Nordeste e Centro-Oeste notificaram um total de 5,9% e 3,3% dos casos, respectivamente (Figura 4) (Brasil, 2023a).

Figura 3- Prevalência global de hepatite Delta.



Porcentagem de sorologia positiva para anti-HDV em indivíduos com sorologia positiva para HBsAg. Fonte: Adaptado de (Stockdale *et al.*, 2020).

Figura 4- Dados Epidemiológicos de casos de hepatite D no Brasil 2000-2022.



Percentual de casos de hepatite D notificados em cada região do Brasil de acordo com notificações entre 2000-2022.

Fonte: Adaptado de (Brasil, 2023a).

No estado do Acre, Dantas (2010) evidenciou que 15,9% dos portadores crônicos do HBsAg apresentavam coinfeção com HDV. Esta taxa se apresenta como muito elevada em comparação a estimativa mundial de 4,5% (Stockdale *et al.*, 2020). Areal (2016) observou uma prevalência de 22,9% de HDV em indivíduos que apresentavam infecção prévia pelo HBV no município de Sena Madureira, no Acre.

1.5 Transmissão e profilaxia da hepatite Delta

A transmissão da hepatite D respeita o mesmo padrão de outras hepatites de transmissão parenteral, sexual e vertical havendo o pré-requisito de infecção prévia ou conjunta ao vírus B, dado a característica única do vírus Delta ser um vírus defectivo, ou seja, não codificar todas as proteínas de sua estrutura (Hughes; Wedemeyer; Harrison, 2011; Koffas; Gill, 2023). Quanto à profilaxia, configuram como principais medidas preventivas a vacinação contra a hepatite B, uso de preservativos, não compartilhamento de objetos de uso pessoal, como lâminas de barbear e depilar, escovas de dente, material de manicure e pedicure, equipamentos para uso de drogas injetáveis, confecção de tatuagem e colocação de *piercings* (Brasil, 2023b; Mentha *et al.*, 2019).

1.6 Doença e evolução clínica da hepatite Delta

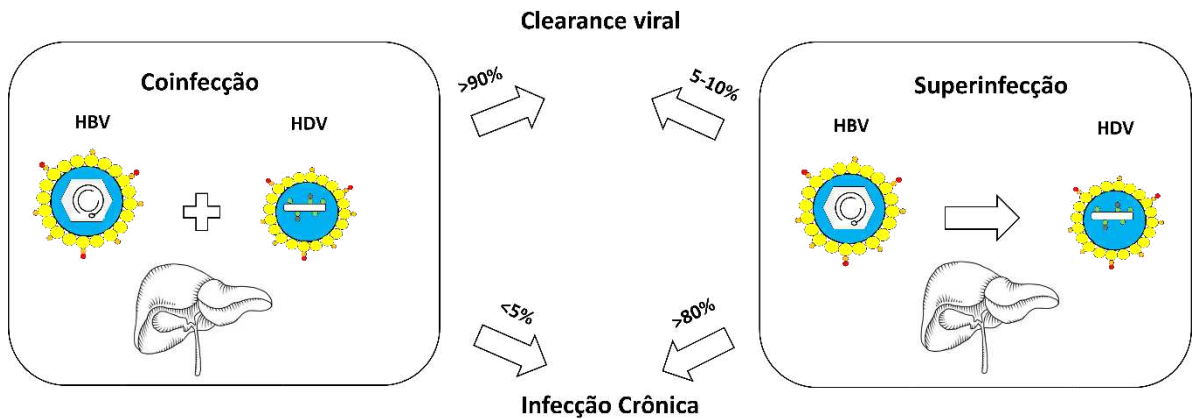
Duas modalidades de infecção pelo HDV são classicamente descritos, coinfeção e superinfecção. A coinfeção ocorre quando o indivíduo adquire ambos os vírus em uma mesma ocasião, apresentando clínica bifásica da doença (Brasil, 2023c). Em um primeiro momento, ocorre a hepatite aguda semelhante às manifestações da infecção pelo HBV isoladamente (Koh; Heller; Glenn, 2019). Após melhora espontânea, novas manifestações de hepatite clínica podem ser observadas, essa última relacionada à expressão sequencial do vírus Delta. A coinfeção HBV/HDV progride para cura espontânea em 90% dos casos, em pacientes adultos, aproximadamente 5% cursam com o dano hepático prolongado da doença crônica (Botelho-Souza *et al.*, 2017; Koh; Heller; Glenn, 2019; Tseligka; Clément; Negro, 2021).

Quando ocorre a infecção pelo vírus da hepatite Delta em pacientes portadores crônicos de HBV define-se uma segunda classificação da doença, a superinfecção. O risco de progressão para doença crônica é aumentado para um percentual maior que 80%, quando comparado à coinfeção, o que aumenta a probabilidade de evoluir para fibrose, descompensação hepática, cirrose e carcinoma hepatocelular (Koh; Heller; Glenn, 2019; Turon-Lagot *et al.*, 2020; Tseligka; Clément; Negro, 2021; Brasil, 2023c) (Figura 5).

Na década de 80, um estudo relatou o caso de cinco pacientes com quadro de hepatite grave, na região de Lábrea, Amazonas. A condição foi posteriormente elucidada, em 1987, com descrição de uma superinfecção pelo vírus da hepatite Delta (Bensabath *et al.*, 1987; Fonseca *et al.*, 1983; Oliveira *et al.*, 2017). As manifestações clínicas da doença em sua condição de hepatite fulminante foram sumarizadas. Documenta-se nesses casos febre, icterícia, dor abdominal, náuseas, vômitos, hepatomegalia, encefalopatia hepática e fenômenos hemorrágicos. Ao mesmo tempo da síndrome clínica, laboratorialmente demonstra-se alterações como linfocitose, e elevação de transaminases pirúvica e oxalacética, atualmente denominada ALT (alanina aminotransferase) e AST (aspartato aminotransferase), que refletem o dano hepatocelular e necrose da massa de hepatócitos, respectivamente. Conjuntamente, eleva-se a bilirrubina direta, o que ilustra a incapacidade de excreção do hepatócito, seguida da ascensão dos níveis de bilirrubina indireta, o que demonstra a incapacidade de conjugação do metabólito por um fígado gravemente acometido (Fonseca *et al.*, 1983; Roulot *et al.*, 2020; Usai *et al.*, 2022).

Quanto às manifestações anatomopatológicas, é demonstrado em exames *post mortem* necrose extensa e difusa do parênquima hepático, corpúsculos hialinos de Councilman, infiltrado denso composto por histiócitos, linfócitos e plasmócitos, principalmente localizados nos espaços porta. Em outras áreas pode-se documentar hepatócitos em degeneração vacuolar, contendo gordura em seu interior, mantendo o núcleo em posição central, células classicamente descritas como em “mórula”, ou “aranha”. Tentativas reparativas esboçam pseudoácinos, que contém em seu interior trombos biliares, e exibem poliploidia. Perda arquitetural das lâminas acinares podem ocorrer pela destruição de fibras reticulares que as sustentam. Sufusões hemorrágicas comumente são visualizadas em perimeio do parênquima hepático inflamado (Fonseca *et al.*, 1983; Fonseca, 2002; Farci; Niro, 2012).

Figura 5- Representação da evolução clínica de paciente com coinfeção e superinfecção por HDV.



A figura representa a infecção pelo vírus do HBV e HDV, à direita a superinfecção e a esquerda o quadro de coinfeção, no centro o percentual de cronificação e resolução da infecção.

Fonte: Adaptado de (Tseligka; Clément; Negro, 2021).

1.7 Diagnóstico

O diagnóstico de hepatite Delta no Brasil, segundo o preconizado pelo Ministério da Saúde, é indicado para indivíduos que apresentem resultados reagentes para o HBsAg em imunoenaios, que sejam provenientes dos estados da região Amazônica, sua progênie ou pessoas que possuam algum vínculo epidemiológico com pessoas desses estados, e também para caso de exacerbação da hepatite B crônica em pacientes com HBV-DNA suprimido (>2.000UI/mL), sem outra etiologia identificada (Brasil, 2023c). O diagnóstico pode ser realizado através da pesquisa de anticorpos anti-HDV, pesquisa de marcadores diretos, pela detecção do genoma viral circulante ou pela detecção do antígeno HDAg, sendo este marcador menos utilizado pela sua detecção transitoriamente no soro do indivíduo, podendo não ser detectado em indivíduos cronicamente infectados (Brasil, 2018; Da; Heller; Koh, 2019).

Marcadores sorológicos são comumente usados na triagem de pacientes, no início da infecção é detectada a IgM anti-HDV, geralmente o marcador aparece entre 2 e 3 semanas após o início dos sintomas e desaparece 2 meses após uma infecção aguda. Em alguns casos pode ocorrer a persistência da infecção por até 9 meses na superinfecção por HDV, este marcador não distingue infecção aguda da crônica, pois há detecção em ambas as fases (Chen *et al.*, 2021). Outro biomarcador é o anticorpo IgG anti-HDV, este pode ser detectado em ambas as fases da infecção podendo ser detectado inclusive após a resolução da infecção (Da; Heller; Koh, 2019). Atualmente, existem testes anti-HDV total disponíveis na rotina de laboratórios biomédicos que são capazes de detectar a IgM e a IgG, como exemplo tem-se o kit LIAISON® XL MUREX

que emprega a tecnologia de quimioluminescência e é licenciado pela ANVISA para uso em laboratório de diagnóstico (Agência Nacional de Vigilância Sanitária, 2023 ; Rocco *et al.*, 2019).

Testes moleculares para a detecção do vírus HDV também estão disponíveis, em especial a RT-PCR quantitativa ou qualitativa, LAMP (Amplificação Isotérmica em alça) (Wang *et al.*, 2013) e PCR digital (Xu *et al.*, 2022), podendo ser uma ferramenta para diagnóstico e monitoramento da infecção por HDV. Existem metodologias desenvolvidas *in house* para detecção molecular e quantificação de carga viral de HDV validadas com amostras clínicas da Amazônia Ocidental, baseada em uma reação em cadeia da polimerase via transcriptase reversa quantitativa (RT-qPCR) (Botelho-Souza *et al.*, 2014). Recentemente, foi desenvolvido um teste quantitativo de apenas um passo experimental para quantificação da carga viral do HDV (Queiroz *et al.*, 2023). O diagnóstico molecular do vírus HDV avançou muito nos últimos anos com desenvolvimento de novas metodologias e empenho da Organização Mundial da Saúde (OMS) que desenvolveu um controle para quantificação do HDV, no entanto, ainda ocorre alta heterogeneidade dos ensaios disponíveis com evidente necessidade de evolução na padronização dos ensaios (Chen *et al.*, 2021; Da; Heller; Koh, 2019; Wang *et al.*, 2013). A necessidade de ampliação da testagem da hepatite Delta na região Amazônica reforça a necessidade de desenvolvimento de testes mais sustentáveis e com redução de custo.

Outro ensaio para detecção de hepatite que pode ser utilizado é a detecção por imunohistoquímica com detecção intra-hepática de HDAg em biópsia hepática. A biópsia hepática de indivíduos com hepatite Delta não apresenta um padrão específico para a doença, podendo ser identificado necrose, inflamação hepatocelular com linfócitos e células de Kupffer infiltrando o parênquima e a região portal. Apesar do padrão histológico ser similar a outras hepatites virais, na hepatite Delta geralmente o quadro tende a ser mais grave. Na doença crônica, a histopatologia consiste em necrose hepatocelular e inflamação no parênquima e região portal, associada a fibrose hepática com severidade diferente, sendo a identificação do HDAg definitivo para o diagnóstico de hepatite D (Botelho-Souza *et al.*, 2017; Chen *et al.*, 2021; Da; Heller; Koh, 2019).

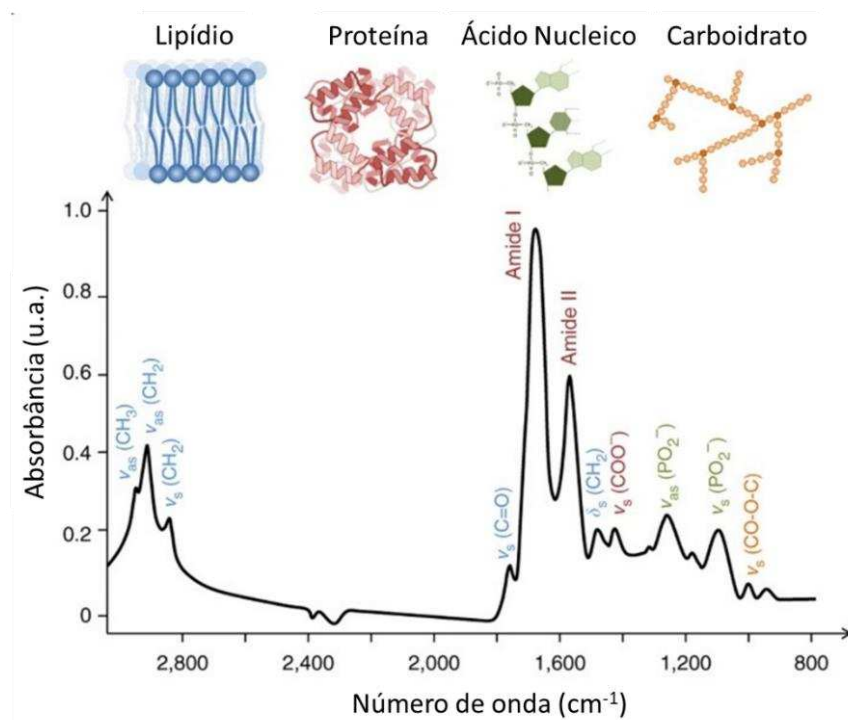
1.8 Espectroscopia no Infravermelho por Transformada de Fourier com Reflectância Total Atenuada (ATR-FTIR)

A técnica de Espectroscopia no Infravermelho por Transformada de Fourier com Reflectância Total Atenuada (ATR-FTIR) é uma técnica que tem se desenvolvido rápido na última década. A plataforma ATR-FTIR apresenta grande potencial para aplicação em triagem, diagnóstico, monitoramento de doenças e prognóstico sem utilização de reagentes, desta forma, apresentando características de sustentabilidade e redução drástica no custo do processamento das amostras. Adicionalmente, esta tecnologia pode ser realizada com procedimentos simplificados para o operador e liberação rápida de resultados com reduzido volume de amostra como saliva, sangue, urina, tecido e células, isto facilita a translação desta tecnologia para serviços públicos e privados de saúde (Caixeta *et al.*, 2020; Fadlelmoula *et al.*, 2022; Lopes *et al.*, 2016; Magalhães; Goodfellow; Nunes, 2021; Naseer; Ali; Qazi, 2021).

O princípio da técnica indica que um feixe de luz infravermelha atinge as amostras e, por consequência, as ligações moleculares que compõem a amostra irão vibrar e alterar o padrão de luz refletido que é mensurado na plataforma de ATR-FTIR. Como a composição de cada amostra difere uma da outra, o ATR-FTIR registra uma impressão digital bioquímica (*fingerprint*) específica da amostra (Baker *et al.*, 2014; Naseer; Ali; Qazi, 2021) (Figura 6). As assinaturas espectrais da amostra podem ser utilizadas para discriminar indivíduos doentes e saudáveis, destacando-se sua aplicação do ATR-FTIR dirigida ao diagnóstico de câncer, doença renal crônica, diabetes mellitus, psoríase, distúrbios neurológicos, bactérias, doenças fúngicas e doenças virais, em especial hepatite B e C (Ali *et al.*, 2021; Ali; Naseer; Qazi, 2022; Caixeta *et al.*, 2020; Naseer; Ali; Qazi, 2021; Roy *et al.*, 2019; Scaglia *et al.*, 2011).

O ATR-FTIR foi utilizado para diferenciar hepatite B e C em amostras de soro humano, os pesquisadores utilizaram três formas de preparo da amostra: i) secagem em uma lamínula de vidro, ii) secagem da amostra direto no cristal ATR; e iii) separação do soro em concentrados de alto peso molecular e baixo peso molecular, com posterior deposição no cristal ATR. A abordagem de separação do soro forneceu a melhor sensibilidade e especificidade, porém foi o método com maior demanda de tempo, o que dificulta sua aplicação em larga-escala. Para diferenciação entre amostras de indivíduos saudáveis de amostras de soro de pacientes infectados com hepatite B (concentrado de alto peso molecular), os valores de sensibilidade e especificidade foram de 87,5% e 94,9%, respectivamente. Com relação a hepatite C *versus* controle o valor de sensibilidade foi de 81,6% e a especificidade de 89,6% (Roy *et al.*, 2019). Este trabalho mostra o potencial uso de ATR-FTIR para diagnóstico de hepatite B e C em soro, sendo esta técnica bastante promissora para diferenciação entre hepatite B e hepatite Delta.

Figura 6- Espectro infravermelho em amostra biológica por meio da plataforma ATR-FTIR.



Espectro de infravermelho do ATR-FTIR indicando modos vibracionais que representam as assinaturas espectrais e suas atribuições biomoleculares (lipídeos, proteínas, carboidratos e ácido nucléico). Azul: lipídeos; Vermelho: proteínas; Verde: ácido nucléico; e Amarelo: carboidrato.

Fonte: Adaptado de (Baker *et al.*, 2014).

A aplicação de ferramentas de inteligência artificial (IA) é uma área que permite desenvolver sistemas computacionais para permitir a resolução de problemas. O termo aprendizado de máquinas é subcampo da IA capaz de automatizar várias tarefas sem intervenção humana desenhado para um objetivo específico. Isto possibilita que a entrada de dados forneça um resultado após treinamento e teste dos algoritmos. O pré-processamento de dados permite modificar os dados por meio de normalizações e remoção de dados irrelevantes para que sejam testadas formas de apresentar o resultado com melhor acurácia. Na fase subsequente, os dados são testados com amostras que não foram utilizadas na fase de pré-processamento para avaliação da classificação gerada pelo algoritmo de IA. Nestes sentido, as avaliações de dados espectrais no infravermelho mais frequentes são: aprendizado de máquinas, análise de componentes principais (PCA), Floresta Randômica e Análise discriminante Linear (LDA) (Fadlelmoula *et al.*, 2023).

1.9 Phage Display

A técnica de *phage display* foi desenvolvida por George P. Smith em 1985, a descrição deste método inovador foi realizada pela fusão da sequência codificante de um peptídeo ao gene pIII do bacteriófago (vírus que infecta bactérias). Isto permitiu que o bacteriófago expressasse o peptídeo na sua superfície de maneira acessível ao reconhecimento de um ligante (Smith, 1985).

Dentre os bacteriófagos de maior relevância empregados na tecnologia de *phage display* estão os filamentos (M13, fd e f1), pois são capazes de infectar bactérias Gram-negativas como *Escherichia coli* (Jaroszewicz *et al.*, 2022). Estes bacteriófagos possuem DNA de fita simples envoltos por um capsídeo constituídos por cinco proteínas (pIII, pVI, pVII, pVIII e pIX) (Jaroszewicz *et al.*, 2022; Tonelli; Colli; Alves, 2013). Das cinco proteínas descritas a proteína pIII (406 resíduos de aminoácidos) e pVIII (50 resíduos de aminoácidos) são mais exploradas nos estudos de expressão de polipeptídios na superfície de bacteriófagos (Hamzeh-Mivehroud *et al.*, 2013; Jaroszewicz *et al.*, 2022). A proteína pIII é eficientemente utilizada para exposição desde peptídeos que geralmente são pequenos, mas podem ter tamanhos maiores com até 38 resíduos de aminoácidos. A proteína pIII é a mais indicada para o isolamento de ligantes com alta afinidade, por outro lado, a proteína pVIII é mais indicada para isolamento de peptídeos curtos com menor afinidade. A proteína pVIII é mais eficiente para exibição de peptídeos menores com até 10 resíduos de aminoácidos (Ebrahimizadeh; Rajabibazl, 2014; Hamzeh-Mivehroud *et al.*, 2013; Jaroszewicz *et al.*, 2022).

O sistema de expressão em bacteriófagos permite a construção de bibliotecas de peptídeos que são utilizadas para rastrear e selecionar peptídeos com alta afinidade às moléculas alvos, sendo o processo de seleção do ligante específico denominado *biopanning* (Jaroszewicz *et al.*, 2022). O primeiro passo do processo é a imobilização da molécula alvo em suporte sólido, podendo ser utilizado placas de microtitulação de poliestireno modificadas ou outras matrizes que permitam a ligação de forma orientada do alvo. Após este processo, a biblioteca de peptídeos de sequências aleatórias de bacteriófagos é colocada em contato com o alvo imobilizado, sendo essa a etapa de seleção biológica por afinidade de ligação ao alvo, neste processo os bacteriófagos não ligantes são removidos, e os bacteriófagos ligantes são eluídos. Os bacteriófagos ligantes são posteriormente amplificados e as etapas de seleção são repetidas entre 3 e 6 vezes para obtenção de um ligante específico, que pode ser caracterizado por sequenciamento (Pande; Szewczyk; Grover, 2010; Smith, 2019).

A tecnologia de *phage display* pode ser aplicada em diversas interfaces de forma bem-sucedida para aplicação em plataformas de diagnóstico. Esta tecnologia foi aplicada no campo da virologia para: influenza suína (Du *et al.*, 2019), vírus da hepatite A do Pato tipo 1 (Xue *et al.*, 2019), Chikungunya (Liu *et al.*, 2019), Zika vírus (Mwale *et al.*, 2020), SARS-CoV-2 (Li *et al.*, 2020), Vírus da encefalite equina venezuelana (Kirsch *et al.*, 2008), vírus da Influenza tipo A (Wu *et al.*, 2011; Yu *et al.*, 2020), Epstein–Barr vírus (Casey *et al.*, 2009), Dengue vírus (Cabezas *et al.*, 2008), hepatite A (Larralde *et al.*, 2007), hepatite C (Pereboeva *et al.*, 2000), hepatite B (Tan; Ho, 2014), entre outros.

2 OBJETIVO

2.1 Objetivo geral

Selecionar e caracterizar biomarcadores por *Phage display* para aplicação em ensaios imunoenzimáticos e desenvolver uma plataforma biofotônica sorológica sustentável suportada por algoritmos de inteligência artificial para detecção de hepatite delta.

2.2 Objetivos específicos

Capítulo I

- Desenvolver uma plataforma biofotônica sustentável suportada por algoritmos de aprendizado de máquinas para detecção hepatite delta em comparação a sujeitos controles e pacientes com hepatite B baseadas em amostras de soro.

Capítulo II

- Desenvolver moléculas miméticas ao HDV por *Phage Display* que reconheçam anticorpos Anti-HDV para desenvolver plataformas de imunodiagnóstico e avaliar os parâmetros de sensibilidade, especificidade e AUC.

CAPÍTULO I

A combined high-throughput, portable and sustainable ATR-FTIR platform for hepatitis D detection in the serum of a large patient cohort from the Brazilian Amazon

Mariana Araújo Costa^{1,2}, Fabiana de Almeida Araújo Santos², Rayany Cristina de Souza^{1,2}, Douglas Carvalho Caixeta^{1,2}, Marco Guevara-Vega^{1,2}, Anagê Calixto Mundim Filho³, Murillo Guimarães Carneiro³, Rafaela Sabatini Melo Pinheiro⁵, Rutilene Barbosa Souza^{5,7}, Ildercílio Mota de Souza Lima⁶, Mario Machado Martins², Thúlio Marquez Cunha³, Luiz Ricardo Goulart^{2,†}, Robinson Sabino-Silva^{1,2*}

¹Innovation Center in Salivary Diagnostics and Nanobiotechnology, Department of Physiology, Institute of Biomedical Sciences, Federal University of Uberlandia, Minas Gerais, Brazil.

²Laboratory of Nanobiotechnology Luiz Ricardo Goulart Filho, Institute of Biotechnology, Federal University of Uberlandia, Minas Gerais, Brazil.

³Faculty of Computing, Federal University of Uberlandia, UFU, MG, Brazil.

⁴Department of Pulmonology, School of Medicine, Federal University of Uberlandia, Minas Gerais, Brazil

⁵Central Laboratory of Public Health of Acre, Secretary of Health of Acre, Acre, Brazil

⁶Laboratory of Applied Molecular and Cellular Biology, Federal University of Acre, Acre, Brazil

⁷Laboratório de Pesquisa e Diagnóstico Molecular em Doenças Infecciosas, Centro de Infectologia Charles Mérieux, Laboratório Rodolphe Mérieux, Acre, Brazil

*Corresponding Author:

Robinson Sabino-Silva; Federal University of Uberlandia (UFU), Innovation Center in Salivary Diagnostics and Nanobiotechnology, Department of Physiology, Institute of Biomedical Sciences (ICBIM), Av. Pará, 1720, Campus Umuruama, CEP 38400-902, Uberlandia, MG, Brazil. Phone: +55 34 3218 2100

E-mail: robinsonsabino@gmail.com

Abstract

Hepatitis Delta (D) is the most severe viral liver disease occurring only in co-infection with the hepatitis B virus (HBV). Hepatitis D presents a higher prevalence in low- and middle-income countries (LMICs). Attenuated total reflectance coupled in Fourier-transform infrared (ATR-FTIR) spectroscopy is a promising alternative for screening and multiple-disease detection. It is imperative to establish high-throughput, portable, sustainable, and low-cost platforms for hepatitis delta virus (HDV) detection. The present study aimed to evaluate the accuracy of this reagent-free biophotonic platform in discriminating hepatitis D (anti-HDV+) patients compared with controls (anti-HBs negative and anti-HBs positive) and hepatitis B patients to be applied as an alternative screening platform for hepatitis D detection. Thus, we evaluated the ATR-FTIR spectrum using 359 blood serum samples evaluated in subjects from the Amazon region of Brazil: 87 controls anti-HBs negative; 94 controls anti-HBs positive; 93 hepatitis B patients; and 85 hepatitis D (anti-HDV+) patients. The support vector machine (SVM) algorithms obtained an accuracy of 80%, 82%, and 74% to discriminate hepatitis D (anti-HDV+) compared with controls anti-HBs negative, controls anti-HBs positive, and hepatitis B patients, respectively. Taken together, the present clinical data highlight the potential of a combined high-throughput, portable, and sustainable ATR-FTIR platform supported with a machine learning algorithm as a screening tool for hepatitis D detection.

Introduction

Hepatitis Delta is the most severe chronic viral hepatitis^{1,2}. Hepatitis D is promoted by the hepatitis D virus (HDV) and this viral infection only occurs in co-infection with the hepatitis B virus (HBV)². Hepatitis D is a global health problem with higher prevalence in low- and middle-income countries (LMICs)²⁻⁴. The declining prevalence of hepatitis D occurs mainly in high-income countries, however, this pattern changed with the emerging prevalence among migrant populations^{2,5}. A significant segment of hepatitis D cases remains unnoticed, the global estimative of hepatitis D prevalence is approximately 5% among the HBV surface antigen (HBsAg) positive population, which represents around 0.16% of the global population or 12 million seropositive HDV patients globally^{3,6}.

HDV is a member of the *Deltavirus* genus in the *Kolmioviridae* family with heterogeneous morphology and around 35 nm in diameter^{7,8}. The HDV genome contains ~1,700 nucleotides, which is insufficient to code viral envelope proteins and replicative enzymes⁸. In this framework, HDV is a single-stranded satellite RNA virus with HBV-dependent

propagation⁹, due to the dependence on HBsAg for its transmission and infectivity⁶. HDV is a defective virus that requires the HBsAg PreS-1 domain of L-HBsAg for its assembly^{2,10}. The HDV infection can occur simultaneously with HBV (coinfection) or sequentially in chronic HBV patients (superinfection)¹¹. Acute coinfection usually leads to self-limited disease¹², however, the progress to chronic diseases in HBV patients was predominant in the superinfection course^{9,10} leading to liver decompensation, liver failure, and faster progression to cirrhosis and hepatocellular carcinoma^{6,13}.

The detection of hepatitis D antibody (anti-HDV) is used as evidence of HDV exposure from immunocompetent subjects, additional molecular diagnostics testing is required to indicate the presence or absence of active HDV infection⁸. The diagnostic methods available for HDV include serological assays applied in the enzyme-linked immunosorbent assay (ELISA) and automated chemiluminescence immunoassays (CLIA), molecular assays to detect HDV RNA in blood samples and liver biopsy^{14,15}. However, these techniques are not widely available in most LMICs and health centers do not investigate coinfection and superinfection, generating unsuitable surveillance national systems for hepatitis D^{3,15,16}. Hepatitis D is a neglected disease, and it is imperative to establish high-throughput, portable, sustainable, and low-cost platforms for HDV detection.

Attenuated total reflection Fourier-transform infrared (ATR-FTIR) spectroscopy is a promising alternative for screening and multiple-disease detection^{17,18}. ATR-FTIR can recognize a wide range of functional groups from lipids, proteins, carbohydrates, and nucleic acids in biological samples¹⁹. ATR-FTIR platform provides advantages compared to other diagnostic or screening methods, it is reagent-free, cost-effective, simple to prepare, rapid to deliver results, and reproducible^{17,18,20}. Most studies that applied ATR-FTIR for disease detection had limitations in the throughput performance with large devices, hence a combined high-throughput, portable, and sustainable ATR-FTIR platform can open new avenues for biophotonic application in public health. The application of FTIR had great results for discriminating patients with hepatitis B and C compared to controls²¹⁻²³, however, in hepatitis D it was not evaluated. Here, we hypothesized that ATR-FTIR can discriminate specific shifts in serological spectra to be used as a screening tool for hepatitis D.

The present study aimed to evaluate the accuracy, sensitivity, and specificity of this reagent-free biophotonic platform to discriminate hepatitis D (anti-HDV+) patients compared with controls anti-HBs negative, controls anti-HBs positive, and hepatitis B patients to be employed as an alternative screening platform for hepatitis D detection.

Material and methods

Ethical Aspects and Study Subjects

The study included 359 blood serum samples provided by the Central Laboratory of Public Health of Acre (LACEN/AC), Rio Branco, Acre, in the Amazon region of Brazil. The samples were classified and codified according to the serological detection or absence of viral hepatitis in four groups: 87 controls anti-HBs negative (subjects without hepatitis B and C with serology negative to anti-HBs, HBsAg, total anti-HBc, and anti-HCV antibodies); 94 controls anti-HBs positive (subjects without hepatitis B and hepatitis C and hepatitis B vaccinated, anti-HBs positive, and negative for HBsAg, total anti-HBc and anti-HCV antibodies) 93 hepatitis B patients (with serology to HBsAg positive and negative for Anti-HDV antibodies); and 85 hepatitis D patients (with positive serology to anti-HDV and previous infection with HBV). All experimental procedures were conducted following ethics statements of the World Medical Association, following the Declaration of Helsinki, and were approved by The Ethical Committee of the Federal University of Uberlandia (UFU) (CAAE #44208621.2.0000.5152).

Sample collection and serology assay

To separate the serum, the blood samples were collected and centrifugated at $3000 \times g$ for 10 minutes. The serum was aliquoted and stored at 2°C - 8°C until serology was performed at the LACEN/AC. Samples were stored at -20°C following the protocols from the fabricant use kit HBsAg for ETI-MAK-4 (DiaSorin, Saluggia, Italy), kit Anti-HBc total for ETI-AB-COREK PLUS (DiaSorin, Saluggia, Italy), anti-HBs for ETI-AB-AUK-3 (DiaSorin, Saluggia, Italy), anti-HCV for MUREUX anti-HCV (versão 4.0) (DiaSorin, Saluggia, Italy) and anti-HDV for ETI-AB-DELTAK-2 (Diasorin, Saluggia, Italy).

ATR-FTIR spectroscopy

A portable ATR-FTIR spectrophotometer coupled with an attenuated total reflectance unit (Agilent Technologies, Agilent Cary 630, Santa Clara, CA, USA) was used for infrared spectra acquisition. The crystal material in the attenuated total reflectance unit is formed by a diamond disc as an internal reflection element. The spectra were analyzed in the wavenumber region from 4000 cm^{-1} to 650 cm^{-1} , and 32 scans were performed per analysis with a resolution of 4 cm^{-1} . Before each serum infrared analysis, the air spectrum was used as a background. For the spectral collection, $10\text{ }\mu\text{L}$ serum samples were applied in a high-throughput system based on aluminum pellets and heated to 80°C in a dry bath (Ageon, Brazil) for ten minutes and added to the ATR crystal.

Data analyses methods

The average spectra of ATR-FTIR were obtained for Orange 3.3.5 software (Bioinformatic Laboratory at the University of Ljubljana, Slovenia). The spectra were normalized, and the baseline was corrected by the Rubberband method. The principal component analysis (PCA) was applied to the spectrum for initial data exploratory analysis using the fingerprint region ($1800 - 900 \text{ cm}^{-1}$).

The average of spectral data of ATR-FTIR was processed by normalization with minimum and maximum methods and baseline correction by Rubberband using the Orange 3.35.0 data mining software (Python 3 programming language).

The infrared spectral analyses performance in the pre-processing and classification stage. The pre-processing stage is divided into aggregation, attribute selection, and data transformation. First, in the aggregation, the average of the three spectral readings of each patient was performed. Next, the spectral data were the fingerprint region ($1800-900 \text{ cm}^{-1}$), in attribute selection. After the Savitzky-Golay smoothing filter was applied to each spectrum followed by a first-order derivative and preprocessed by amide I normalization.

The classification was tested with cutting-edge feature extraction tools coupled to machine learning algorithms. The Linear Discriminant Analysis (LDA) and Support Vector Machine (SVM) were selected based on better results during model training. The analyses were performed with ten times and stratified using cross validation in both LDA and SVM algorithms to evaluate the predictive performance based on sensitivity, specificity, and accuracy. The sensitivity or true positive rate is the proportion of positives (anti-HDV positive) that were correctly classified, and the specificity or true negative rate is the proportion of negatives (controls for each analysis) that were correctly classified. The accuracy is defined as the total number of samples correctly classified considering true and false negatives²⁰.

Results

1.1. Analyses of the ATR-FTIR.

A mean infrared spectra obtained from serum of hepatitis D (anti-HDV+) patients, controls anti-HBs negative, controls anti-HBs positive, and hepatitis B patients (Fig. 1). Analysis of the spectra showed difference between the hepatitis D (anti-HDV+) patients and the controls anti-HBs negative, controls anti-HBs positive, and hepatitis B patients, supposed it is a distinct molecular profiles among each spectral class.

The PCA was applied in mean infrared spectra to find low dimensional data by projecting the data into linear subspaces and detecting potential infrared spectral changes in

hepatitis D (anti-HDV+) patients comparing with controls anti-HBs negative, controls anti-HBs positive, and hepatitis B patients. The two principal components (PC1 and PC2) explained 87.72% of the cumulative variance comparing hepatitis D (anti-HDV+) patients with controls anti-HBs negative (Fig. 2A). PC1 and PC2 explained 87.24% of the cumulative variance between hepatitis D (anti-HDV+) patients with controls anti-HBs positive (Fig. 2B). PC1 and PC2 explained 89.89% of the cumulative variance between hepatitis D (anti-HDV+) patients and hepatitis B patients (Fig. 2C).

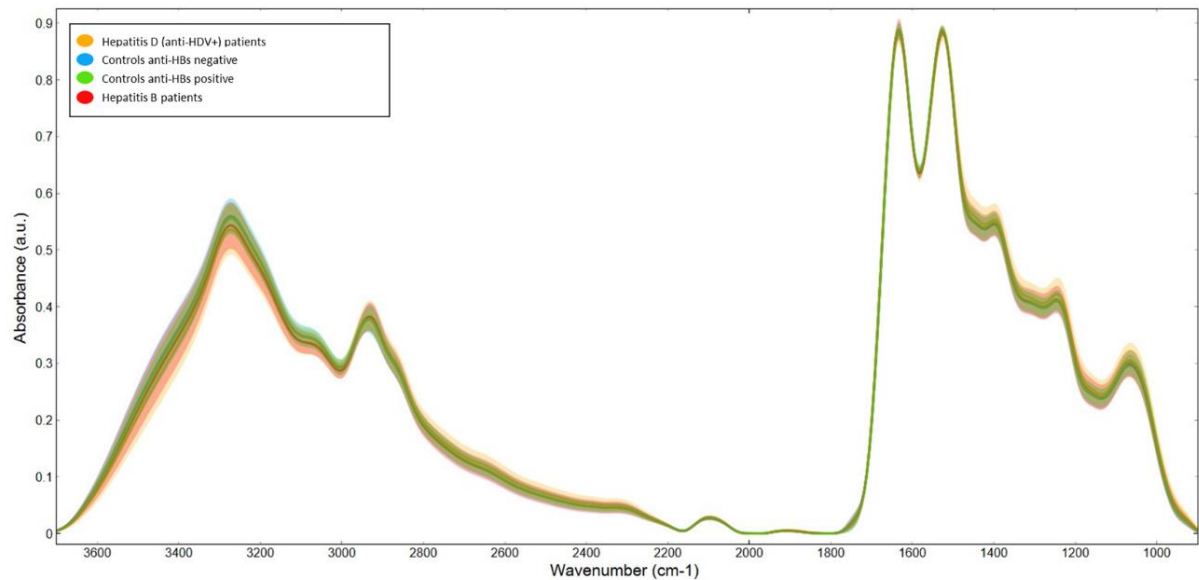


Figure 1. Representative average of serum infrared spectra of hepatitis D (anti-HDV+) patients, controls anti-HBs negative, controls anti-HBs positive, and hepatitis B patients.

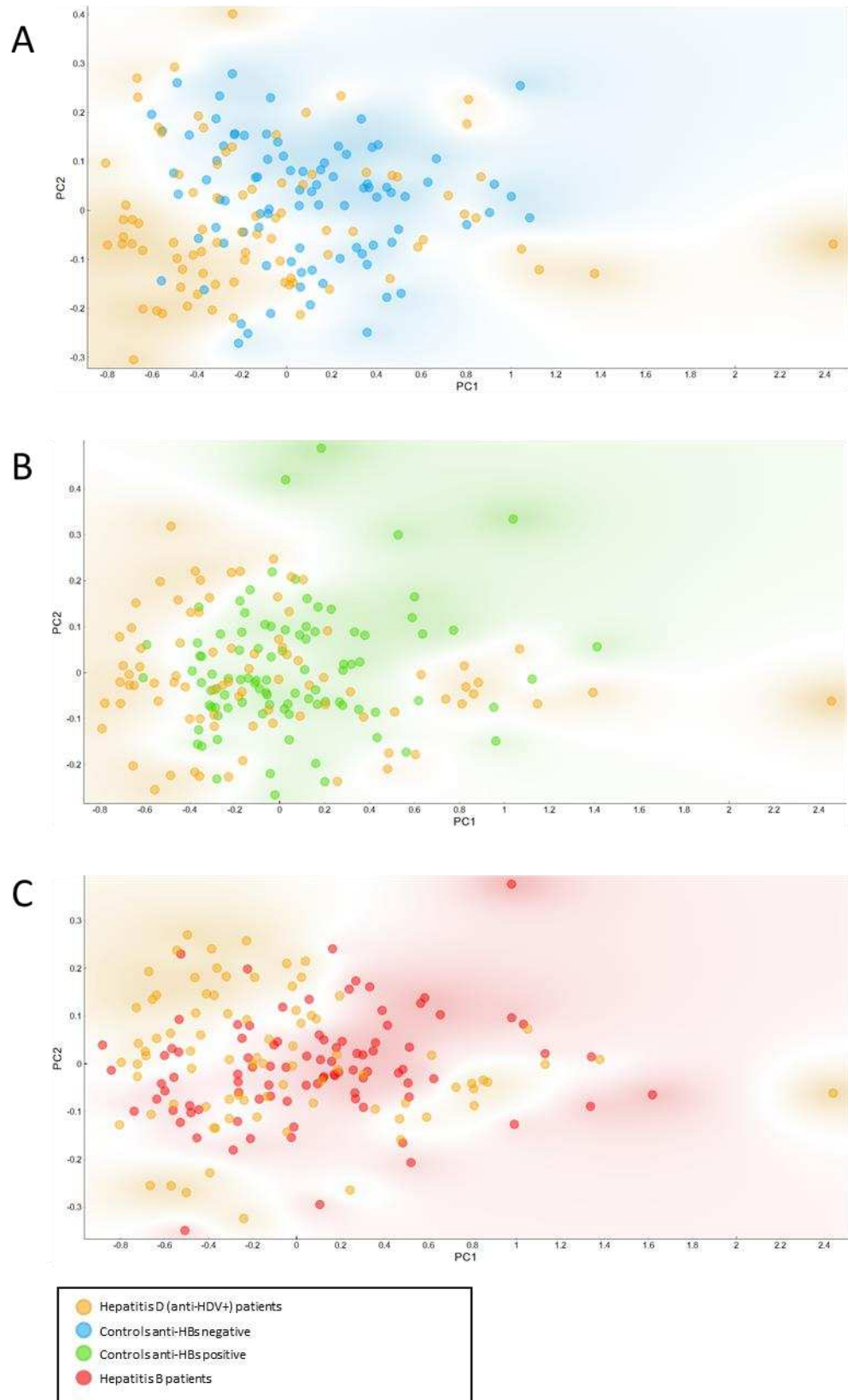


Figure 2. Principal Component Analysis PC1 vs. PC2 from serum infrared spectra from hepatitis D (anti-HDV+) patients compared with (A) controls anti-HBs negative (B) controls anti-HBs positive (C) hepatitis B patients.

In order to classify and discriminate serum infrared spectra from hepatitis D (anti-HDV+) patients, hepatitis B patients, controls anti-HBs positive and controls anti-HBs negative in an automated protocol, a learning machine approach was applied using linear discriminant analysis (LDA) and support vector machine (SVM) are described in Table 1-3. The result obtained in these analyses indicates that the best discrimination between controls anti-HBs negative compared to hepatitis D (anti-HDV+) was performed by the SVM algorithm followed by Amide I normalization using (1800-900 cm^{-1}). This classification of serum spectra by the SVM algorithm showed a sensitivity of 79%, specificity of 82%, and accuracy of 80% comparing controls anti-HBs negative with hepatitis (anti-HDV+) patients. The best result to discriminate patients with serology positive for hepatitis D (anti-HDV+) from controls anti-HBs positive was the SVM algorithm following the Savitzky-Golay smoothing filter with Amide I normalization using (1800-900 cm^{-1}). The classification of serum spectra by the SVM algorithm showed a sensitivity of 80%, specificity of 85%, and accuracy of 82% to discriminate between hepatitis (anti-HDV+) patients and controls anti-HBs positive. The best results for discrimination of hepatitis B and hepatitis D (Anti-HDV+) was the SVM algorithm followed Polinomial Correction using (1800-900 cm^{-1}) and Asymmetric least squares (ALS) baseline using (1800-900 cm^{-1}). The classification of serum spectra by the SVM algorithm showed a sensitivity of 71%, specificity of 77%, and accuracy of 74% for both tests to discriminate anti-HDV positive and hepatitis B patients.

Table 1. Machine learning algorithms applied in serum blood spectra to discriminate controls anti-HBs negative to hepatitis D (anti-HDV+)

Pre-Processing	Algorithm	Accuracy	Sensitivity	Specificity
Raw data (1800 - 900 cm^{-1})	Linear Discriminant Analysis	0,73	0,72	0,74
	Support Vector Machine	0,79	0,77	0,8
Amide I norm (1800 - 900 cm^{-1})	Linear Discriminant Analysis	0,72	0,67	0,76
	Support Vector Machine	0,8	0,79	0,82
Savgolay+Amide I (1800 - 900 cm^{-1})	Linear Discriminant Analysis	0,74	0,7	0,78
	Support Vector Machine	0,79	0,8	0,79
Polinomial Correction (1800-900 cm^{-1})	Linear Discriminant Analysis	0,79	0,76	0,82
	Support Vector Machine	0,8	0,8	0,8
ALS + Savgolay (1800 - 900 cm^{-1})	Linear Discriminant Analysis	0,79	0,76	0,82
	Support Vector Machine	0,78	0,8	0,76
Rubberband (1800-900 cm^{-1})	Linear Discriminant Analysis	0,73	0,68	0,77
	Support Vector Machine	0,78	0,8	0,76

Table 2. Machine learning algorithms applied in serum blood spectra to discriminate controls anti-HBs positive and hepatitis D (anti-HDV+)

Pre-Processing	Algorithm	Accuracy	Sensitivity	Specificity
Raw data (1800 - 900cm ⁻¹)	Linear Discriminant Analysis	0,74	0,71	0,78
	Support Vector Machine	0,8	0,76	0,83
Amide I norm (1800 - 900cm ⁻¹)	Linear Discriminant Analysis	0,72	0,67	0,77
	Support Vector Machine	0,82	0,79	0,84
Savgolay+Amide I (1800 - 900cm ⁻¹)	Linear Discriminant Analysis	0,79	0,74	0,83
	Support Vector Machine	0,82	0,8	0,85
Polinomial Correction (1800 - 900 cm ⁻¹)	Linear Discriminant Analysis	0,8	0,74	0,85
	Support Vector Machine	0,8	0,77	0,83
ALS (1800 - 900cm ⁻¹)	Linear Discriminant Analysis	0,8	0,77	0,84
	Support Vector Machine	0,82	0,79	0,85
Rubberband (1800 - 900 cm ⁻¹)	Linear Discriminant Analysis	0,71	0,68	0,74
	Support Vector Machine	0,81	0,77	0,83

Table 3. Machine learning algorithms applied in serum blood spectra to discriminate hepatitis B patients and hepatitis D (anti-HDV+)

Pre-Processing	Algorithm	Accuracy	Sensitivity	Specificity
Raw data (1800 - 900cm ⁻¹)	Linear Discriminant Analysis	0,68	0,66	0,7
	Support Vector Machine	0,68	0,65	0,71
Amida, I norm (1800 - 900cm ⁻¹)	Linear Discriminant Analysis	0,67	0,63	0,7
	Support Vector Machine	0,7	0,69	0,71
Savgolay+Amide I (1800 - 900cm ⁻¹)	Linear Discriminant Analysis	0,68	0,63	0,72
	Support Vector Machine	0,71	0,66	0,76
Polinomial Correction (1800 - 900 cm ⁻¹)	Linear Discriminant Analysis	0,72	0,64	0,78
	Support Vector Machine	0,74	0,71	0,77
ALS (1800 - 900cm ⁻¹)	Linear Discriminant Analysis	0,69	0,62	0,74
	Support Vector Machine	0,74	0,71	0,77
Rubberband (1800 - 900 cm ⁻¹)	Linear Discriminant Analysis	0,66	0,61	0,69
	Support Vector Machine	0,73	0,71	0,75

Shapley Addite Explanations (SHAP) is a model for the explainability of artificial intelligence. This is a technique determining the relative significance of features in the model²⁴ of discrimination between hepatitis D (anti-HDV+) patients compared with controls anti-HBs negative, controls anti-HBs positive, and hepatitis B patients to be employed as an alternative screening platform for hepatitis D detection. The model gives Shapely Values which calculate the contribution of each feature to the target value. We applied SHAP values to select the most important vibrational modes responsible for discrimination by the best algorithm between hepatitis D (anti-HDV+) patients compared to control groups.

The SHAP feature importance indicates the main serum blood vibrational modes at 1466 cm^{-1} , 1468 cm^{-1} , 1421 cm^{-1} , 1464 cm^{-1} , 1077 cm^{-1} , 1574 cm^{-1} , 1056 cm^{-1} , 1498 cm^{-1} , 1075 cm^{-1} , 1660 cm^{-1} , as responsible for distinguishing controls anti-HBs negative from hepatitis D (Anti-HDV+) patients (Fig. 3). The vibrational modes at 1649 cm^{-1} , 1462 cm^{-1} , 1464 cm^{-1} , 1682 cm^{-1} , 1628 cm^{-1} , 1634 cm^{-1} , 1489 cm^{-1} , 1684 cm^{-1} , 1541 cm^{-1} , 1472 cm^{-1} were responsible for distinguishing controls anti-HBs positive from patients with serology positive for anti-HDV (Fig. 4). The vibrational modes at 1628 cm^{-1} , 1626 cm^{-1} , 1462 cm^{-1} , 1675 cm^{-1} , 1649 cm^{-1} , 1654 cm^{-1} , 1610 cm^{-1} , 1544 cm^{-1} , 1664 cm^{-1} , 1498 cm^{-1} were responsible for distinguishing hepatitis B patients and from hepatitis D (anti-HDV+) patients (Fig. 5). The molecular assignments of each vibrational mode indicated by SHAP feature analysis were described in Table 4²⁵⁻²⁷.

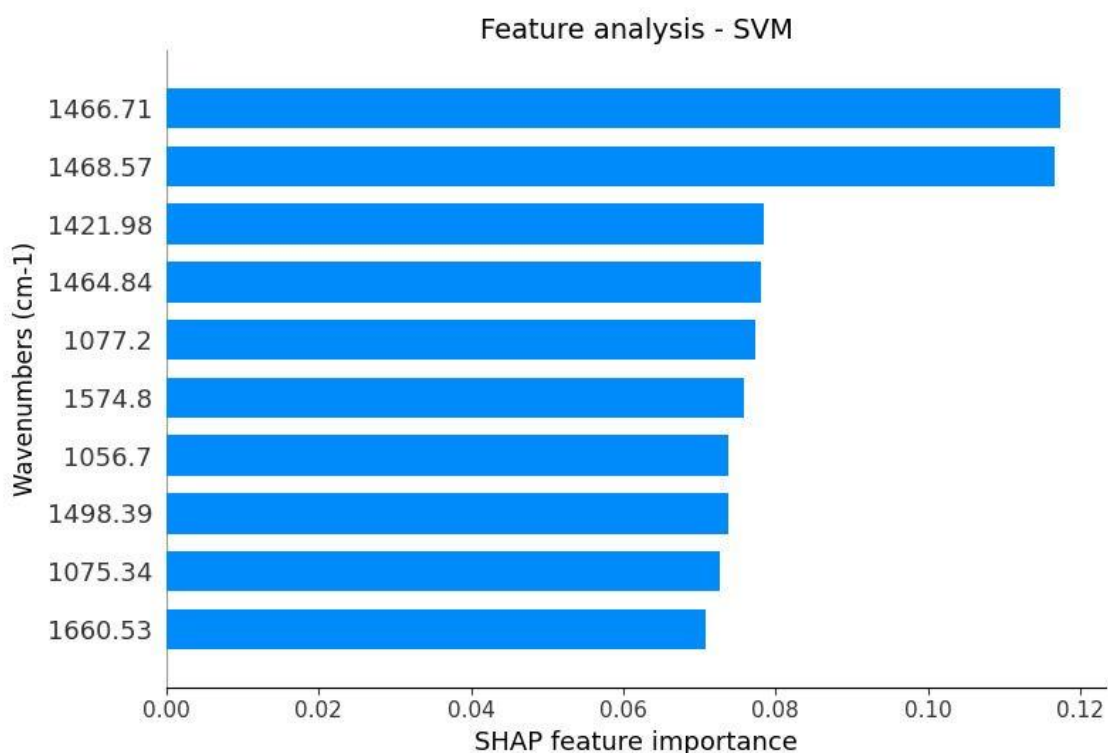


Figure 3. The feature importance (SHAP value) graph of SVM model applied to discriminate controls anti-HBs negative and hepatitis D (anti-HDV+).

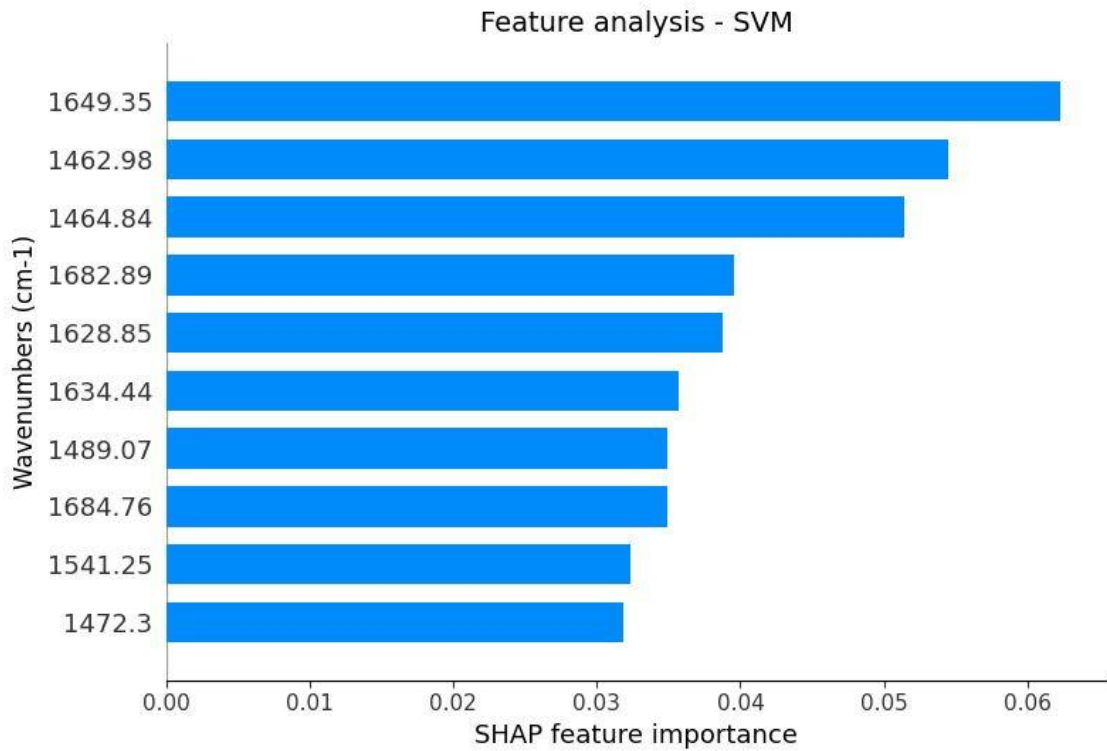


Figure 4. The feature importance (SHAP value) graph of SVM model applied to discriminate controls anti-HBs positive and hepatitis D (anti-HDV+).

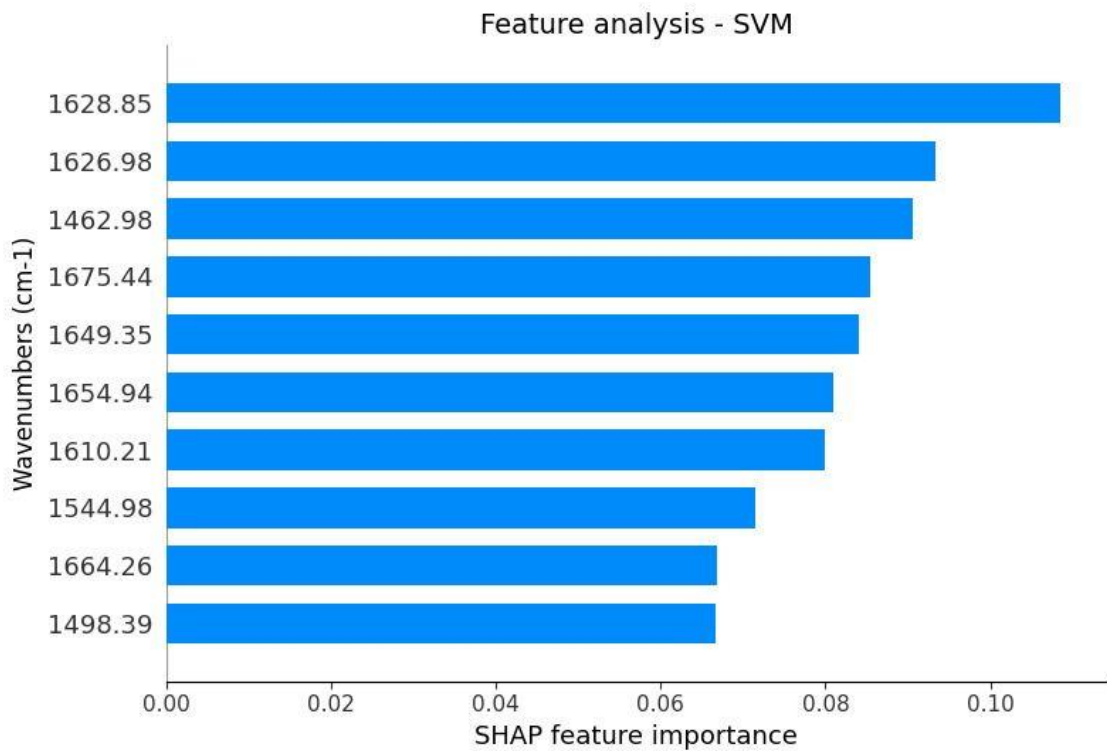


Figure 5. The feature importance (SHAP value) graph of SVM model applied to discriminate hepatitis B patients and hepatitis D (anti-HDV+).

Table 4. The tentative assignments for loading plots to the best-performing spectral vibrational modes selected for discriminate hepatitis D (anti-HDV+) patients from control anti-HBs negative, control anti-HBs positive, and hepatitis B patients.

Wavenumber	Band assignment	Biomolecular components
1466 cm ⁻¹	CH ₂ scissoring mode of the acyl chain	Lipid
1468 cm ⁻¹	δ CH ₂	Lipid
1421 cm ⁻¹	$\nu_s(\text{COO}^-)$	Carbohydrates
1464 cm ⁻¹	CH ₂ scissoring mode of the acyl chain	Lipid
1077 cm ⁻¹	C-O and C-C stretching and C-O-H deformation motions	Carbohydrates
1574 cm ⁻¹	Amide II	Protein
1056 cm ⁻¹	ν C-O & δ C-O	Carbohydrates
1498 cm ⁻¹	Amide II (an N-H bending vibration coupled to C-N stretching)	Protein
1075 cm ⁻¹	Absorption due to C-O and C-C stretching and C-O-H deformation motions	Carbohydrates
1660 cm ⁻¹	Amide I band	Protein
1649 cm ⁻¹	Unordered random coils and turns of amide I	Protein
1462 cm ⁻¹	δ_{as} CH ₃	Protein
1682 cm ⁻¹	Unordered random coils and turns of amide I	Protein
1628 cm ⁻¹	Amide I region	Protein
1634 cm ⁻¹	β -sheet structure of amide I	Protein
1489 cm ⁻¹	ν [COO ⁻]	Protein
1684 cm ⁻¹	Amide I (disordered structure-non-hydrogen bonded)	Protein
1541 cm ⁻¹	Amide II absorption (primarily an N-H bending coupled to a C-N stretching vibrational mode)	Protein
1472 cm ⁻¹	CH ₂ bending of the methylene chains	Lipids
1626 cm ⁻¹	Amide I region	Protein
1675 cm ⁻¹	Amide I (anti-parallel β -sheet)	Protein
1654 cm ⁻¹	Amide I (of proteins in α -helix conformation)	Protein
1610 cm ⁻¹	β -sheets (hydrogen bonds)	Protein
1544 cm ⁻¹	Amide II bands (C-N stretching & CHN bending vibrations)	Protein
1664 cm ⁻¹	Amide I	Protein

Discussion

The detection of hepatitis D in a portable and high-throughput platform can be a suitable alternative to offer adequate and early treatment, it is profitable to reduce the impact of progressive viral damage in the liver, cirrhosis, morbidity, and mortality²⁸. The application of a portable and simple-to-operate platform for hepatitis D detection can also reduce public health costs and improve quality of life. HDV diagnostics are not widely available in most geographical hotspots with higher HDV infection prevalence. In this context, the development of a combined high-throughput, portable, and sustainable ATR-FTIR platform to detect unique changes in serum components of hepatitis D and differentiate its spectra from healthy controls and hepatitis B has great potential to be applied in decentralized resource-limited laboratory settings and contribute to translation of biophotonics into the clinic.

The detection level of total anti-HDV antibodies is considered adequate for hepatitis D diagnosis. The Enzyme-linked immunosorbent tests are extensively used and provide highly accurate results. However, this analysis requires a long time to deliver results and for this diagnostic test and requires the use of toxic and costly reagents, which is inadequate for hepatitis D surveillance in low- and middle-income countries (LMICs)²⁹.

As a way of graphically visualizing the distribution of data, PCA demonstrated a moderate distinction between the groups with the main information present in PCA1 and PCA2. The potential to distinguish serum infrared spectra was analyzed with an application of pre-processing protocol in the biofingerprint region to develop tools to be used in the detection of hepatitis D in large-scale cohorts and clinical practice, we use selected regions of the spectrum ($1800-900\text{ cm}^{-1}$) with the presence of organic components to a classification process by machine learning algorithms.

The infrared spectra of serum are a unique biomolecular signature of multiple components and present broad-spectrum markers with the potential to be used in a diagnostic perspective from healthy subjects patients with, or without, hepatitis D co-infection. From the point of view of the screening application, this large-scale discovery study developed a sustainable biophotonic platform supported by machine learning algorithms to discriminate hepatitis D (anti-HDV+) patients from healthy controls anti-HBs negative with a sensitivity of 79%, specificity of 82%, and accuracy of 80%. This platform also discriminates hepatitis D (anti-HDV+) patients from control anti-HBs positive subjects with a sensitivity of 80%, specificity of 85%, and accuracy of 82%. Besides, this sustainable biophotonic platform also performed detection of hepatitis D (anti-HDV+) patients from hepatitis B patients; with a

sensitivity of 71%, specificity of 77%, and accuracy of 74%. The application of this unique SVM algorithm in serum infrared spectra is a pioneer tool for the diagnosis of hepatitis D. These SVM algorithms assembled to detect hepatitis D are a potential candidate for HDV portable screening in remote undeveloped communities in the Amazon region of Brazil or other low- and middle-income countries (LMICs), where other enzymatic chemiluminescence or real-time PCR tests are not disposal.

The SHAP with the SVM algorithm showed specific vibrational modes that contributed to the distinction between the patients with hepatitis D and healthy subjects with or without anti-HBs detection. The vibrational modes that mostly contributed to the discrimination of hepatitis D (Anti-HDV+) patients from control subjects (anti-HBs negative) were 1466 cm^{-1} , 1468 cm^{-1} are related to lipid. The SHAP features indicate the vibrational mode at 1649 cm^{-1} , which is related to protein, as the main responsible component to discriminate hepatitis D (Anti-HDV+) patients from control subjects (anti-HBs positive). The vibrational mode that mostly contribute to the discrimination of hepatitis D (Anti-HDV+) patients from hepatitis B patients was the 1628 cm^{-1} , which is also related to a protein component.

The HDV infection had a worse prognosis than other hepatitis in clinical events^{30,31}, this findings are consistent with the decompensation metabolic of HDV. The hepatitis viruses cause normally altered lipid profiles, decreased cholesterol levels, and serum lipid concentrations, the host lipid metabolism, particularly cholesterol metabolism, is required for the hepatitis viral infection and life cycle³². Additionally, the Brazilian study of hepatitis D patients in Brazilian Western Amazonia analyzed clinical and metabolic aspects comparing hepatitis B and superinfected with HDV they found a high proportion of clinical alteration with hepatitis D patients, such as hematologic alterations anemia, thrombocytopenia and thrombocytosis and the hepatologic markers ALT, AST and serum bilirubin³³. The results show that ATR-FITR is capable of detecting changes in metabolism compatible with HDV infection. Consequently, employing ATR-FITR presents a potential avenue for a cost-effective detection that can economically optimize the screening processes, thereby mitigating complications associated with HDV.

A recent study showed that samples containing low molecular weight components of blood applied in ATR-FTIR spectroscopy analysis present a sensitivity of 69.4% and specificity of 83.3% comparing hepatitis B patients and control subjects. This study also showed that ATR-FTIR detected hepatitis C in patients than control subjects with a sensitivity of 68% and specificity of 80.3%. It was suggested that ATR-FTIR can be used to detect blood serum

changes promoted by hepatitis B virus and hepatitis C virus, however, this study does not focus on the analysis of hepatitis D as the present study²².

Based on the estimative of the impact of several forms of hepatitis worldwide, it was suggested that novel global strategies should be urgently implemented to improve screening access to viral hepatitis³⁴. In this context, with further additional development, the present proposed platform tested in this large population-based with healthy subjects, vaccinated subjects, hepatitis B patients, and hepatitis D patients could have a significant impact on the screening detection of hepatitis D and also for discrimination between hepatitis B with or without hepatitis D co-infection.

From a translational perspective, hepatitis delta detection is of paramount relevance to optimize medical strategies with current treatment options. The early diagnostics based on HDV and the detection with antibodies against the HDV exhibit low availability in public health services of low- and middle-income countries. This sustainable biophotonic platform provides a pan-omic spectroscopy analysis that is potentially capable of detecting simultaneously viral components (peptides, proteins, lipids) and unique immunological factors against viral infection (proteins, lipids, carbohydrates, nucleic acids) enabling the timely detection of hepatitis D. The application of this large-scale green technology is suitable to be included in public and private healthcare systems due to its minimal sample preparation with rapid results and cost-effective option. Furthermore, this photonic bioanalytical platform supported by learning machine algorithms offers a label-free and sustainable hepatitis D detection with ultra-low sample volume. This could be crucial for conducting tests in riverine communities of the Amazon, given the high prevalence of hepatitis D, even though testing rates remain low. Additionally, this sustainable platform can be especially profitable in the Amazon region due to the potential impact of current tests on environmental contamination. Besides, our platform described here can be applied for triage of symptomatic patients or assembled with real-time PCR, ELISA, and lateral flow assays as orthogonal tests.

Conclusion

Here, we showed that learning machine analyses were used in a combined high-throughput, portable, and sustainable ATR-FTIR platform for hepatitis D detection. The classification of this biophotonic platform in a large patient cohort from Brazilian Amazon using serum blood samples comparing hepatitis D (anti-HDV+) patients with control subjects with anti-HBs negative, control subjects with anti-HBs positive, and hepatitis B patients

showed, respectively, 80%, 82%, and 74% accuracy by SVM algorithm. Taken together, the present data highlight the potential of a combined high-throughput, portable, reagent-free, and sustainable ATR-FTIR platform coupled with a machine learning algorithm as a screening tool for hepatitis D.

ADDITIONAL INFORMATION

Competing financial interests

The funders had no role in the design of the study; in the collection, analyses, or interpretation of data; in the writing of the manuscript; or in the decision to publish the results. The results presented in this manuscript are related with patent application: Costa, M.A.; Santos, F.A.A.S.; Caixeta, D.C.; Guevara-Vega, M.; Carneiro, M.G.; Mundim, A.C Martins M.M.; Cunha, T.M.; Goulart, L.R. are present in the filled patente “DETECÇÃO DE HEPATITE DELTA BASEADO EM MODOS VIBRACIONAIS INFRAVERMELHOS ACOPLADOS EM ALGORITMO DE INTELIGÊNCIA ARTIFICIAL”, 2023. Registration number: BR 1020230228500. Date of deposit: 31/10/2023.”.

Authors' contributions

M.A.C., L.R.G., F.A.A., R.S-S, I.M.S.L, M.G.C conceptualization; M.A.C., R.S.M.P., R.B.S. sample acquisition; M.A.C., R.C.S., D.C.C. performed the experiments; M.A.C., R.C.S., D.C.C., M.G.V., R.S.M.P., R.B.S., I.M.S.L., A.C.M., M.M.M., T.M.C., analyzed the data; L.R.G., T.M.C., M.G.C., A.C.M., R. S-S. resource; M.A.C, FA.A.S., R.C.S., D.C.C., M.G.V., M.G.C., R.S.M.P., R.B.S., I.M.S.L, A.C.M., M.M.M., T.M.C., R.S-S., wrote the paper.

Acknowledgments

Gratitude to Professor Dr. Luiz Ricardo Goulart who led the beginning of the work and unfortunately due to COVID-19 could not be present to see the final work.

We also thank Greiciele Carvalho Leite, Janaína Mazaro, Janete Taynã Nascimento Rodrigues, Camilo Matheus Monteiro Braga de Oliveira, Francilene de Oliveira Braz, Carmen Silva dos Santos Silva, they support the research at Central Laboratory of Public Health of Acre, Secretary of Health of Acre, Acre, Brazil.

REFERENCES

1. Cunha, C., Tavanez, J. P. & Gudima, S. Hepatitis delta virus: A fascinating and neglected pathogen. *WJV* **4**, 313 (2015).
2. Caviglia, G. P., Ciancio, A. & Rizzetto, M. A Review of HDV Infection. *Viruses* **14**, (2022).
3. Stockdale, A. J. *et al.* The global prevalence of hepatitis D virus infection: Systematic review and meta-analysis. *J Hepatol* **73**, 523–532 (2020).
4. Miao, Z. *et al.* Estimating the Global Prevalence, Disease Progression, and Clinical Outcome of Hepatitis Delta Virus Infection. *J Infect Dis* **221**, 1677–1687 (2020).
5. Stroffolini, T. *et al.* Migratory flow and hepatitis delta infection in Italy: A new challenge at the beginning of the third millennium. *J Viral Hepat* **27**, 941–947 (2020).
6. Ghany, M. G. A Glimmer of Hope for an Orphan Disease. *N Engl J Med* **389**, 81–82 (2023).
7. Walker, P. J. *et al.* Changes to virus taxonomy and to the International Code of Virus Classification and Nomenclature ratified by the International Committee on Taxonomy of Viruses (2021). *Arch Virol* **166**, 2633–2648 (2021).
8. Asselah, T. & Rizzetto, M. Hepatitis D Virus Infection. *N Engl J Med* **389**, 58–70 (2023).
9. Hughes, S. A., Wedemeyer, H. & Harrison, P. M. Hepatitis delta virus. *The Lancet* **378**, 73–85 (2011).
10. Sagnelli, C. *et al.* HBV/HDV Co-Infection: Epidemiological and Clinical Changes, Recent Knowledge and Future Challenges. *Life (Basel)* **11**, (2021).
11. Smedile, A. *et al.* INFLUENCE OF DELTA INFECTION ON SEVERITY OF HEPATITIS B. *The Lancet* **320**, 945–947 (1982).
12. Caredda, F. *et al.* Hepatitis B Virus-Associated Coinfection and Superinfection with Agent: Indistinguishable Disease with Different Outcome. *Journal of Infectious Diseases* **151**, 925–928 (1985).
13. Tseligka, E. D., Clément, S. & Negro, F. HDV Pathogenesis: Unravelling Ariadne's Thread. *Viruses* **13**, (2021).
14. Da, B. L., Heller, T. & Koh, C. Hepatitis D infection: from initial discovery to current investigational therapies. *Gastroenterology Report* **7**, 231–245 (2019).
15. Ceesay, A. *et al.* Viral Diagnosis of Hepatitis B and Delta: What We Know and What Is Still Required? Specific Focus on Low- and Middle-Income Countries. *Microorganisms* **10**, 2096 (2022).
16. Kumar, P. *et al.* Needs of Individuals Living With Hepatitis Delta Virus and Their Caregivers, 2016-2019. *Prev Chronic Dis* **17**, E159 (2020).

17. Fadlelmoula, A., Pinho, D., Carvalho, V. H., Catarino, S. O. & Minas, G. Fourier Transform Infrared (FTIR) Spectroscopy to Analyse Human Blood over the Last 20 Years: A Review towards Lab-on-a-Chip Devices. *Micromachines* **13**, 187 (2022).
18. Magalhães, S., Goodfellow, B. J. & Nunes, A. FTIR spectroscopy in biomedical research: how to get the most out of its potential. *Applied Spectroscopy Reviews* **56**, 869–907 (2021).
19. Baker, M. J. *et al.* Using Fourier transform IR spectroscopy to analyze biological materials. *Nat Protoc* **9**, 1771–1791 (2014).
20. Caixeta, D. C. *et al.* Salivary molecular spectroscopy: A sustainable, rapid and non-invasive monitoring tool for diabetes mellitus during insulin treatment. *PLoS ONE* **15**, e0223461 (2020).
21. Ali, S., Naseer, K., Hussain, I. & Qazi, J. ATR-FTIR spectroscopy-based differentiation of hepatitis C and dengue infection in human freeze-dried sera. *Infrared Physics & Technology* **118**, 103912 (2021).
22. Roy, S., Perez-Guaita, D., Bowden, S., Heraud, P. & Wood, B. R. Spectroscopy goes viral: Diagnosis of hepatitis B and C virus infection from human sera using ATR-FTIR spectroscopy. *Clinical Spectroscopy* **1**, 100001 (2019).
23. Ali, S., Naseer, K. & Qazi, J. Diagnosis of HCV infection using attenuated total Reflection-FTIR spectra of Freeze-Dried sera. *Infrared Physics & Technology* **121**, 104019 (2022).
24. Srinivasu, P. N., Sandhya, N., Jhaveri, R. H. & Raut, R. From Blackbox to Explainable AI in Healthcare: Existing Tools and Case Studies. *Mobile Information Systems* **2022**, 1–20 (2022).
25. Chaber, R. *et al.* A Preliminary Study of FTIR Spectroscopy as a Potential Non-Invasive Screening Tool for Pediatric Precursor B Lymphoblastic Leukemia. *Molecules* **26**, 1174 (2021).
26. Movasaghi, Z., Rehman, S. & ur Rehman, Dr. I. Fourier Transform Infrared (FTIR) Spectroscopy of Biological Tissues. *Applied Spectroscopy Reviews* **43**, 134–179 (2008).
27. Luo, Y. *et al.* Diagnostic segregation of human breast tumours using Fourier-transform infrared spectroscopy coupled with multivariate analysis: Classifying cancer subtypes. *Spectrochimica Acta Part A: Molecular and Biomolecular Spectroscopy* **255**, 119694 (2021).
28. Koh, C., Heller, T. & Glenn, J. S. Pathogenesis of and New Therapies for Hepatitis D. *Gastroenterology* **156**, 461-476.e1 (2019).
29. Rocco, C. *et al.* Comparison of anti-hepatitis D virus (HDV) ETI-AB-DELTA-2 assay and the novel LIAISON® XL MUREX anti-HDV assay in the diagnosis of HDV infection. *Diagn Microbiol Infect Dis* **95**, 114873 (2019).
30. Palom, A. *et al.* Long-term clinical outcomes in patients with chronic hepatitis delta: the role of persistent viraemia. *Aliment Pharmacol Ther* **51**, 158-166 (2020).

31. Roulot, D. Origin, HDV genotype and persistent viremia determine outcome and treatment response in patients with chronic hepatitis delta. *Journal of Hepatology* **73**, (2020).
32. Liou, J.-W., Mani, H. & Yen, J.-H. Viral Hepatitis, Cholesterol Metabolism, and Cholesterol-Lowering Natural Compounds. *Int J Mol Sci* **23**, (2022).
33. de Oliveira, M. S. & Silva, R. P. M. Hepatitis B and Delta: clinical aspects of patients in the Brazilian Western Amazonia. *Rev Bras Enferm* **72**, 1265-1270 (2019)
34. Cui, F. *et al.* Global reporting of progress towards elimination of hepatitis B and hepatitis C. *Lancet Gastroenterol Hepatol* S2468-1253(22)00386–7 (2023)
doi:10.1016/S2468-1253(22)00386-7.

CAPÍTULO II

Novel Epitope-Based Diagnostic Probes Selected by Phage Display for Serological Detection of HDV

Mariana Araújo Costa^{1,2,3}, Rayany Cristina de Souza^{1,2}, Tércio Peixoto Roca⁴, Adrhyan Araújo da Silva Oliveira^{4,5}, Bruno Silva Andrade⁶, Luiz Felype Alves de Souza⁷, Rutilene Barbosa Souza⁷, Rafaela Sabatini Melo Pinheiro^{3,8}, Iara Pereira Soares¹, Marco Guevara-Vega^{1,2}, Douglas Carvalho Caixeta^{1,2}, Ildercílio Mota de Souza Lima⁸, Ana Máisa Passos-Silva^{4,5}, Mario Machado Martins¹, Abel Dib Rayashi¹, Daniel Archimedes da Matta⁷, Deusilene Vieira⁵, Luiz Ricardo Goulart^{1†}, Robinson Sabino-Silva^{1,2}, Fabiana de Almeida Araújo Santos¹.

¹Laboratory of Nanobiotechnology Prof. Dr. Luiz Ricardo Goulart Filho, Institute of Biotechnology, Federal University of Uberlandia, Minas Gerais, Brazil.

²Innovation Center in Salivary Diagnostics and Nanobiotechnology, Department of Physiology, Institute of Biomedical Sciences, Federal University of Uberlandia, Minas Gerais, Brazil.

³Central Laboratory of Public Health of Acre, Secretary of Health of Acre, Acre, Brazil.

⁴Laboratory of Viral Hepatitis, Oswaldo Cruz, FIOCRUZ, Rio de Janeiro, Brazil.

⁵Laboratory of Molecular Virology, Oswaldo Cruz Foundation of Rondônia- FIOCRUZ/RO, Porto Velho, Brazil.

⁶Laboratory of Bioinformatics and Computational Chemistry, Department of Biological Sciences, State University of Southwest of Bahia (UESB), Jequié, Bahia, Brazil.

⁷Centro de Infectologia Charles Merieux & Laboratório Rodolphe Merieux (FUNDHACRE), Rio Branco, Brazil.

⁸Laboratory of Applied Molecular and Cellular Biology, Federal University of Acre, Acre, Brazil.

Running title:

Correspondence to: Fabiana de Almeida Araújo Santos

Instituto de Biotecnologia da Universidade Federal de Uberlândia, Uberlândia, IBTEC, Av.

Pará, 1720, Campus Umuruama, CEP 38400-902, Uberlândia, MG, Brazil

Phone: + 55 34 996430025

E-mail: fabiana.aasantos@gmail.com

Abstract

HDV is a satellite virus with infectivity and transmission only in subjects with chronic hepatitis B virus (HBV) infection. HDV infection is related to faster progression to cirrhosis and hepatocellular carcinoma. There is a considerable lack of testing for HDV especially in developing countries where HDV is endemic. The *Phage display* employs high-affinity molecules that effectively interact with targets, offering potential application in innovative diagnostic systems with high accuracy and cost-effectiveness. Here, we develop HDV mimetic molecules recognized by anti-HDV antibodies using *Phage Display* technology for application in HDV immunodiagnostic platforms. Based on the sequence of peptides selected, we constructed a recombinant protein HDAgProt to be applied in enzyme-linked immunoassay (ELISA) presenting a sensitivity of 74.71%, a high specificity of 97.85%, and an AUC: 0.8906. In the analysis of patients with active infection, the detection parameters were improved presenting a sensitivity of 88.0%, specificity of 98.92%, and area under the curve (AUC) of 0.96. In this context, the application of HDAgProt in an ELISA assay was effective to discriminate between hepatitis D patients and hepatitis B mono-infection patients, highlighting the potential use in another's efficient, fast, portable, and low-cost platforms for HDV detection.

Introduction

Hepatitis delta virus (HDV) is a small spherical virus, a member of the *Kolmioviridae* family, with a negative single-stranded circular RNA genome that exclusively encodes the HDAg protein. This protein can be presented in two forms small (S-HDAg) and large (L-HDAg)¹⁻⁴. The virus envelope is composed of HBsAg a protein of hepatitis B virus (HBV) a single biological property². HDV is often classified as a satellite virus of hepatitis B virus (HBV), due to its inefficiency to complete its replication cycle in the absence of HBV^{5,6}. There are eight HDV subtypes with high diversity containing inter-genotype homology ranging from 80-85% and distinct geographic distribution. In this context, the HDV-1 genotype is the most prevalent genotype globally and it is thought to be the precursor of all the other genotypes. The HDV-3 genotype, which is found only in South America, exhibits the most significant divergence compared to the other genotypes⁷⁻⁹. The global prevalence of HDV remains uncertain. When it was estimated based on anti-HDV tests in individuals with positive serology for HBsAg, the suggested prevalence was 48-60 million HDV-infected patients worldwide. However, other data accepted by the World Health Organization (WHO) recently suggested 12 million HDV-infected patients worldwide⁹⁻¹¹.

The chronic hepatitis D infection is the worst prognosis of viral hepatitis, presents a high risk of developing liver cirrhosis, hepatocellular carcinoma, and liver-related death¹²⁻¹⁵. The two forms of HDV infection depend on how the infection is acquired: the co-infection occurs simultaneously with HBV infection and the super-infection occurs in an HBV carrier¹⁶. Simultaneous infection usually leads to acute self-limited hepatitis, the majority of immunocompetent patients will eliminate both diseases, and less than 5% will develop the chronic infection^{12,13,17}. On the other side, super-infection, results in chronic HDV-HBV infection in more than 90% of infected patients, and it is associated with a swift progression leading to the development of liver cirrhosis^{14,17}.

As a general approach, the laboratory diagnosis of HDV infection includes the detection of antigens and/or antibodies by enzyme immunoassays or chemiluminescence assays, followed by molecular tests to detect HDV RNA by real-time PCR^{18,19}. Ideally, HDV protocol for diagnostic testing is required for all patients with chronic HBV infection^{20,21}. Although mandatory, there is a considerable lack of testing for HDV in chronic HBV-infected patients, especially in developing countries where HDV is endemic, due to a lack of resources¹⁸, a fact that can lead to underestimation of hepatitis delta diagnosis²¹, this highlights the critical importance of formulating alternative tools for screening HDV.

Phage display is a technology that applies a combinatorial library of bacteriophages that express a high variability of peptides that bind to specific targets through intermolecular interaction, providing peptides of high affinity and specificity^{22,23}. The selection process is called biopanning which removes low-affinity molecules and selects molecules with high-affinity bindings^{24,25}. Bacteriophages with high affinity can be amplified and characterized by sequencing to identify their peptide sequences²⁴. In this context, our aim was to select and synthesize HDV mimetic molecules recognized by anti-HDV antibodies using *Phage Display* technology for application in an immunoenzymatic platform for hepatitis delta detection.

Methods

Sample characterization and Ethical aspects

All the procedures follow the ethics guidelines and regulations. Two hundred blood serum samples were selected from a public diagnosis laboratory in the Amazon (north region of Brazil) at the Central Laboratory of Public Health of Acre (LACEN-AC). The laboratory classified and codified all samples according to the serologic status of viral hepatitis: Group 1 – HBsAg, anti-HBc total, anti-HBs, anti-HCV, negative (10 samples); Group 2 – HBsAg, anti-HCV, anti-HBc total negative and positive anti-HBs positive (10 samples); Group 3 (HBV

Control) – HBsAg positive and anti-HDV negative (93 samples): and Group 4 (anti-HDV+) – HBsAg and anti-HDV positive (87 samples). The Ethics Committee of the Federal University of Uberlândia approved this project (CAAE: #44208621.2.0000.5152).

Phage Display

Coupling of IgGs in protein G magnetic beads

To start the Phage Display selection cycles, we employed the system of magnetic protein G-coupled Dynabeads (Life Technologies Corporation®, Carlsbad, CA, USA) for the IgG antibodies coupling. The protocol was performed following the manufacturer's guidelines, with some modifications. The 2×10^9 bead particles (100 μ L of the stock) were washed 3 times with phosphate-buffered saline (PBS) for the activation of microspheres. Then, 100 μ L of pool samples, with 10 μ L of 10 patients, from each group of participants (Group 1, Group 2, Group 3, Group 4) were added to 4 different tubes and incubated under agitation for 40 minutes at room temperature. The antibody-adsorbed beads were separated on a magnet stand (DynaMag™, Washington Mills North Grafton, Inc., North Grafton, MA, USA) to discard the supernatant (non-binding antibodies). The attached beads were subsequently washed 3 times in PBS with 0.05% Tween 20 (PBS-T 0.05%) to remove non-binding antibodies.

Biopanning

The biopanning involved the selection and amplification of HDV mimetic peptides. For selection, 10 μ L of viral suspension (2×10^{11} phages) from a Ph.D.-C7C library of phage-fused peptides (New England Biolabs, Beverly, MA, USA) was diluted in 190 μ L of PBS-T 0.1% to select ligands for IgG from HDV-positive patients. The phage library is composed of 7 random amino acids expressed in the pIII region of the bacteriophage, flanked by a pair of cysteine residues forming a disulfide bond during phage assembly. Selection was performed with 20 μ L of protein G microspheres bound immunoglobulins from the 4 different groups. For this purpose, three negative selections were performed, the phage library was successively

incubated (30 minutes at room temperature) with pooled samples of Group 1, and the unbound phage particles transferred to pooled samples of Group 2 and Group 3, followed by positive selection with pooled samples of anti-HDV + Group 4. Then, the beads were washed 10 times with PBS-T 0.1% and the supernatant was discarded. The acid elution was performed by adding 500 μ L of 0.2 M glycine (pH 2.2), incubated for 10 minutes, the supernatant was removed and neutralized with 75 μ L of Tris- HCl (pH 9.1). After the selection phase, the elutes were amplified using the *E. coli* ER2738 strain (New England Biolabs, Beverly, MA, USA) and purified with 20% polyethylene glycol (PEG)/2.5 M NaCl, suspended in PBS. Three rounds of biopanning were performed. After each round, the titration was done to determine the input and output of viral particles during the selection cycle. For all titrations, 1.0 μ L of phages were used, diluted in 9.0 μ L of LB culture medium. Dilutions 10^{-1} to 10^{-4} were made for non-amplified eluates and 10^{-8} to 10^{-11} for amplified phages. The dilutions were incubated with 200 μ L of *E. coli* ER2738 strain in mid-log phase (OD₆₀₀~ 0.5) for 5 minutes and plated in Luria-Bertani (LB) medium containing 840 mM isopropyl β -D-1-thiogalactopyranoside (IPTG) and 49 mM 5-bromo-4-chloro-3-indolyl β -D-galactopyranoside (X-gal), with 3.0 mL of Top Agar. After incubation, for 18 hours at 37°C, the phage-infected *E. coli* ER2738 colonies are visualized in blue²³ (Fig. 1).

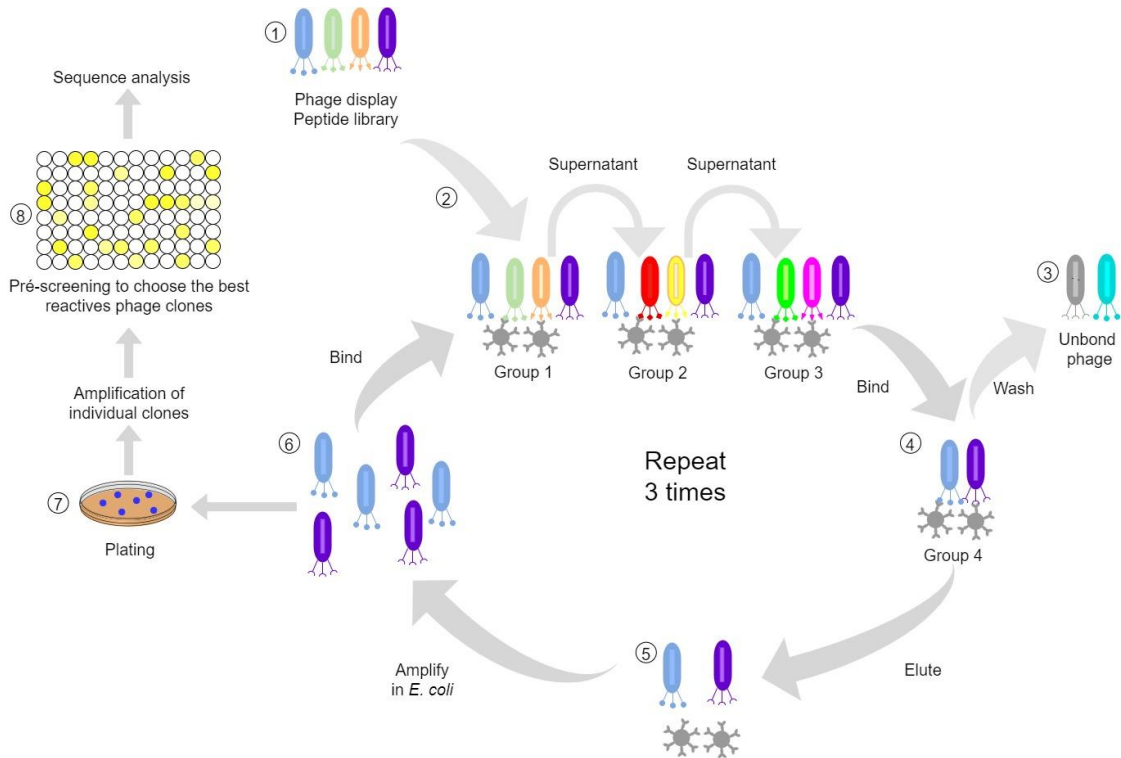


Figure 1. A scheme of biopanning. (1) The phage library was incubated with Dynabeads™ protein G with antibodies (IgG) and was performed sequentially, (2) with 3 negative and one positive selection. (3) Unbound phages were washed (4) and those recognized by anti-HDV antibodies (IgG) bead Dynabeads™ (5) were eluted (6) and amplified in *E. coli* ER2738, for three rounds. (7) The eluted phages were plated, collected, and amplified (8) to select the best reactive phage clones by ELISA and sequence analysis.

DNA extraction and sequencing of phages

The phages of 3^o titration were isolated and put to grow at deepwell containing 1.2 mL of early-log-phase ER2738 culture (OD₆₀₀ ~0.03) overnight. The DNA extraction was performed as previously described^{23,26}. The DNA of selected phages was submitted to DNA sequencing using BigDye® Terminator v3.1 Cycle Sequencing Kit on ABI 3730xl Genetic Analyzer (Applied Biosystems, Foster City, California) at *BPI Biotecnologia*® (Botucatu, São Paulo, Brazil). The peptide sequences were deduced according to the nucleotide sequences and analyzed using ExPASy translate (<https://web.expasy.org/translate/>).

Phage-ELISA

ELISA assay was performed to analyze the reactivity of clones with IgGs from anti-HDV + patients against hepatitis B Control. Microtiter plates (NUNC Maxisorp) were coated with 1:500 anti-M13 monoclonal antibody (GE Healthcare), diluted in 50mM bicarbonate buffer (pH 9.6) for 16 hours at 4°C. After the plates were washed (PBS) and blocked with 3% BSA PBS-T 0.05%, for 1 hour at 37°C. Then, the plates were washed 3 times with PBS-T 0.05% and incubated with phage supernatant for 1 hour at 37°C. Subsequently, the plates were washed 6 times and then incubated with a pool of serum from hepatitis B Control patients and anti-HDV+ diluted 1:100 in PBS-T 0.05%, for 1 hour at 37°C. Again, plates were washed six times and incubated with anti-IgG human conjugated with horseradish peroxidase (HRP) (1:5000). After 6 washes, antigen/antibody binding was detected by adding ortho-phenylenediamine (OPD) buffer at 1 mg/mL with 3% H₂O₂ (Sigma Chemical Co.). The reaction was halted with the addition of 4N sulfuric acid. Reactivity was measured using a plate reader at 492nm. The most promising phages were submitted to another round of phage ELISA employing serum from individual patients (10 positives and 10 negatives from hepatitis D). We also assessed two blocking agents (BSA or skimmed milk) and serum dilution (1:100, 1:250, and 1:500) and two different phage concentrations 10¹⁰ and 10¹¹ pfu/well.

Peptide design and synthesis

The sequencing phage clones were aligned using Clustal Omega²⁷ to the L-HDAg sequence, which is a protein of HDV, obtained from GenBank (AVO03797.1) for the design of synthetic peptide. Also, the antigenicity of B-cell from the L-HDAg sequence was analyzed using Linear Epitope prediction 2.0^{28,29} to identify the epitope regions (<http://tools.iedb.org/bcell/help/>). The epitope regions that aligned with the best reactivity clones were chosen for the design of the peptide sequences. When aligning the clone sequences with the L-HDAg protein, several clones aligned in the same region, so we used the native sequence of the protein to design the 3 synthetic peptides, performed by GenScript USA Inc.

(Piscataway, NJ, USA). The peptide HDAg1 (ACKDGEGAPCGGGSAETVES), HDAg2 (ACMEVDSGPCGGGSAETVES), HDAg3 (KDGEGAPPAKRARTDQMEVDSGP). The HDAg1 and HDAg2 were constructed with 20 residues, both containing a disulfide bridge (between residues 2-10), acylation in the N-terminal, and amidation in the C-terminal. The HDAg3 was constructed with 23 residues, acylation in the N-terminal, and amidation in the C-terminal, without a disulfide bridge.

3 D modeling

The large hepatitis delta antigen (L-HDAg) sequence (AVO03797.1) was submitted to the artificial intelligence (AI) tool trRosetta server (<http://yanglab.nankai.edu.cn/trRosetta/>), for 3D modeling³⁰. In addition, we submitted the same sequence to the protein homology modeling server Phyre2 (<http://www.sbg.bio.ic.ac.uk/phyre2/html/page.cgi?id=index>) which was used as a template for the 1A92 crystal structure from the oligomerization domain of the L-HDAg³¹. In addition, both structures generated by AI and homology tools were structurally aligned for identifying conserved domains using the software Pymol 2.5 (Schrödinger, LLC.). After that, the two peptide sequences (HDAg1 and HDAg2) were submitted to a three three-dimensional homology against the 3D modeling (trRosetta) of L-HDAg using The Pepitope Server (<http://pepitope.tau.ac.il/>).

Recombinant protein design, expression and purification

The HDAgProt was synthesized using the pET-22b(+) cloning vector by GenOne Biotech (Rio de Janeiro, Brazil) constructed from the L-HDAg virus protein sequence of portion 63-118 aa with 12,4 kDa. The plasmid was transformed into *E. coli* BL21 (DE3) pLysS cell and incubated on a Luria-Bertani (LB) agar plate containing 100 µg/mL ampicillin overnight at 37°C. A single colony from this plate was used to inoculate a 10 mL LB culture (100 µg/mL ampicillin), which was grown for 12 h at 37°C, 250 rpm. The overnight culture was used to inoculate 600 mL of LB (100 µg/mL ampicillin) and incubated to grow to an optical density of

0.600 (OD=0.8). After the growth, we added 1mM IPTG and incubated for 5 hours at 37°C, 250 rpm. We collected the cells by centrifugation (3,500 x g for 15 min, 4 °C) and resuspended them in PBS with 0.25% lysozyme. The cells were lysed by thermal shock and sonication under 0.55 cycles, 55% amplitude for 30 seconds, 3 times. After sonication, the cells were centrifuged at 10,000 x g at 4 °C, for 30 minutes. Then, the supernatant was discarded and urea buffer (8 M of urea and 25 mM of Tris-HCl pH 8.0) was added to the precipitated cells. Next, centrifuged at 10,000 x g, at 4°C, for 20 minutes and discarded the precipitated. The supernatant was purified on HPLC (Shimadzu, Kyoto, Japan) and quantified in SDS-PAGE gel using the ImageJ program, with BSA (1 mg/mL) as a reference.

ELISA using synthetic peptides and recombinant protein

A first ELISA with the synthetic peptides (HDAg1, HDAg2, HDAg3) was performed to evaluate the better conditions for serum dilution (1:100, 1:250) and peptides dilution (200 ng/well and 1 µg/well). For this, an ELISA plate (Greiner, Frickenhausen, Germany) was coated in duplicate with HDAg1, HDAg2, and HDAg3, diluted with carbonate buffer (0.1 M NaHCO₃, pH 8.6) overnight at 4 °C. After washing (PBS-T 0.05%) and blocking (PBS-T 0.05% with skimmed milk 5%) for 1 hour. The plate was incubated for 1 h at 37 °C with individual sera (1:100 and 1:250 in PBS-T 0.05%). The wells were washed 6 times followed by incubation with anti-IgG human HRP (GE Healthcare) diluted (1:5000) in PBS-T 0.05% for 1 h at 37 °C. The plate was washed 6 times and revealed with OPD SigmaFast™ (Sigma-Aldrich) and read at 492 nm. Another ELISA protocol was carried out to compare the reactivity of the HDAg3 and HDAgProt from anti-HDV+ (87 samples) and HBV controls (93 samples). An ELISA plate was coated in duplicate HDAg3 (200 ng/well) and HDAgProt (0.05 µg/well), diluted with carbonate buffer (0.1 M NaHCO₃, pH 8.6) overnight at 4 °C. After washing (PBS-T 0.1%) and blocking (PBS-T 0.1% with skimmed milk 5%) for 1 hour. The plate was incubated for 1 h at 37 °C with individual sera (1:250 in PBS-T 0.1%). The wells were washed 6 times followed by

incubation with anti-human IgG HRP (GE Healthcare) and anti-human IgM (μ -chain specific) HRP (Sigma-Aldrich) diluted (1:5000) in PBS-T 0.1% for 1 h at 37 °C. The plate was washed 6 times and revealed with OPD SigmaFast™ (Sigma-Aldrich) and subsequent readings were taken at 492 nm.

RNA HDV detection and sequencing

The total nucleic acids were extracted using 100 μ L of serum on the Loccus Extracta 32 equipment (Loccus, Brazil) using the manufacturer's instruction. The detection of HDV was performed with the RT-qPCR reaction described previously³². The cycle thresholds (Cts) were analyzed and the samples who was ≤ 30 for the viral target were selected for sequencing protocol. The sequencing protocol was performed, and the first step was made cDNA assays with SuperScript III Two Step (Invitrogen). To characterize the HDV genotype, a Nested-PCR was used, containing newly synthesized cDNA in a PCR mix with primers previously described in the literature that amplify a 406 bp fragment of the HDV genome corresponding to the application of the Delta antigen³³. The PCR products were analyzed in gel electrophoresis (2% agarose) at 100V for 30 minutes together with a 100 bp DNA ladder. After the gel was analyzed, it was purified using ExoSAP (Cellco, New York, NY, USA). The purified product was used for sequencing using the SeqStudio automated sequencer (Applied Biosystems, Waltham, MA, USA).

Statistical analysis

The reactivity with ratio was calculated between the absorbances of the positive-HDV and control. To determine the difference among groups for peptides and recombinant protein reactivity, the data was non-normally distributed data, we used the unpaired t-test with Mann-Whitney. In addition, sensitivity, specificity, cut-off, and AUC parameters were calculated based on ROC curve analysis. All analyses were performed using GraphPad Prism 7 software

(GraphPad Software, Inc. San Diego, CA). Values of $p < 0.05$ were considered significant and the results were expressed as mean \pm S.D.

Results

Phage-ELISA and Sequence Analysis

After 3 rounds of biopanning, 80 samples presented valid sequences (without sequence errors) with 46 unique sequences (Table 1). The 46 phages were submitted to an immunoreactivity test by phage-ELISA (Fig. 2). It was observed that some clones exhibited substantial reactivity, with a reactivity ratio ranging from 2-3 in 25 of the clones when comparing absorbances from pooled samples of anti-HDV+ patients to HBV control patients. Additionally, 6 clones demonstrated a reactivity ratio of ≥ 3 .”

Clones	Sequence	Frequency clones
HD1	KQEDGGP	1/80
HD2	KDAMGGP	5/80
HD3	RNEDGGP	3/80
HD4	QQEDGGP	18/80
HD5	NRDHRIQ	1/80
HD6	KDNTGGP	1/80
HD7	PRQEDGG	1/80
HD8	MNESFPG	1/80
HD9	KDEFGAY	3/80
HD10	SKQEDGG	2/80
HD11	SKEATPF	1/80
HD12	KDEHAGS	1/80
HD13	KEDQRGQ	1/80
HD14	TSEDGGP	1/80
HD15	KDGAGGP	2/80
HD16	DTTLHLG	2/80
HD17	KDSVSGP	1/80
HD18	KDNPGGP	1/80
HD19	KDAVGGP	4/80
HD20	KDSVAGP	1/80
HD21	YLHGYGT	1/80

HD22	LWWEKPT	1/80
HD23	LWWEKQK	1/80
HD24	LWWQTHL	1/80
HD25	RSDDGGP	2/80
HD26	KAYPYLK	1/80
HD27	RDSHRL	1/80
HD28	DTTUSDN	1/80
HD29	KEDHVG	1/80
HD30	QQEDGGH	1/80
HD31	KDDAGGP	3/80
HD32	KDEYGAY	1/80
HD33	NSHRHGA	1/80
HD34	DTTLTWF	1/80
HD35	KDESGSY	1/80
HD36	TQKEPAW	1/80
HD37	RYDDGGP	1/80
HD38	MSTDNNY	1/80
HD39	KDGSGGP	1/80
HD40	MEEDGGP	1/80
HD41	LTDVRGA	1/80
HD42	KEGHECQ	1/80
HD43	LWWEQSR	1/80
HD44	KDGLAGP	1/80
HD45	KDPGAGP	1/80
HD46	SRIQMLH	1/80

Table 1. Sequence and frequency of phage clones.

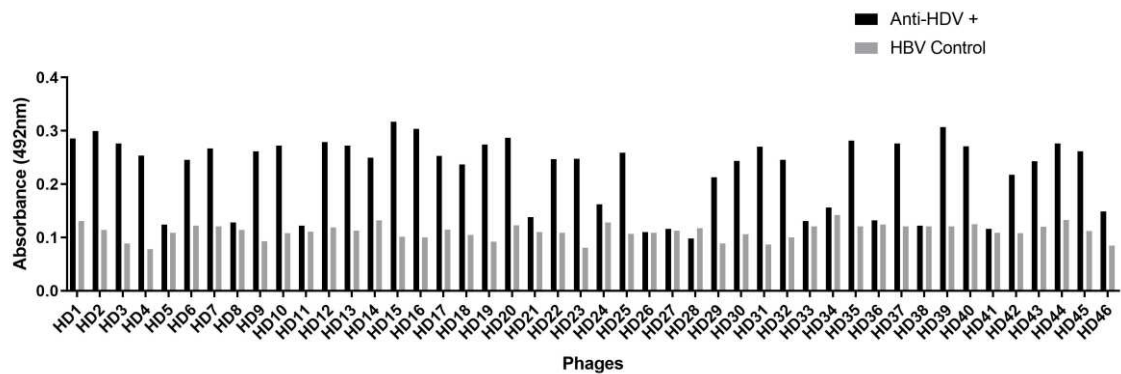


Figure 2. Phage-ELISA with 46 selected phage clones in biopanning with two serum pools from 10 anti-HDV+ samples and 10 HBV Control samples.

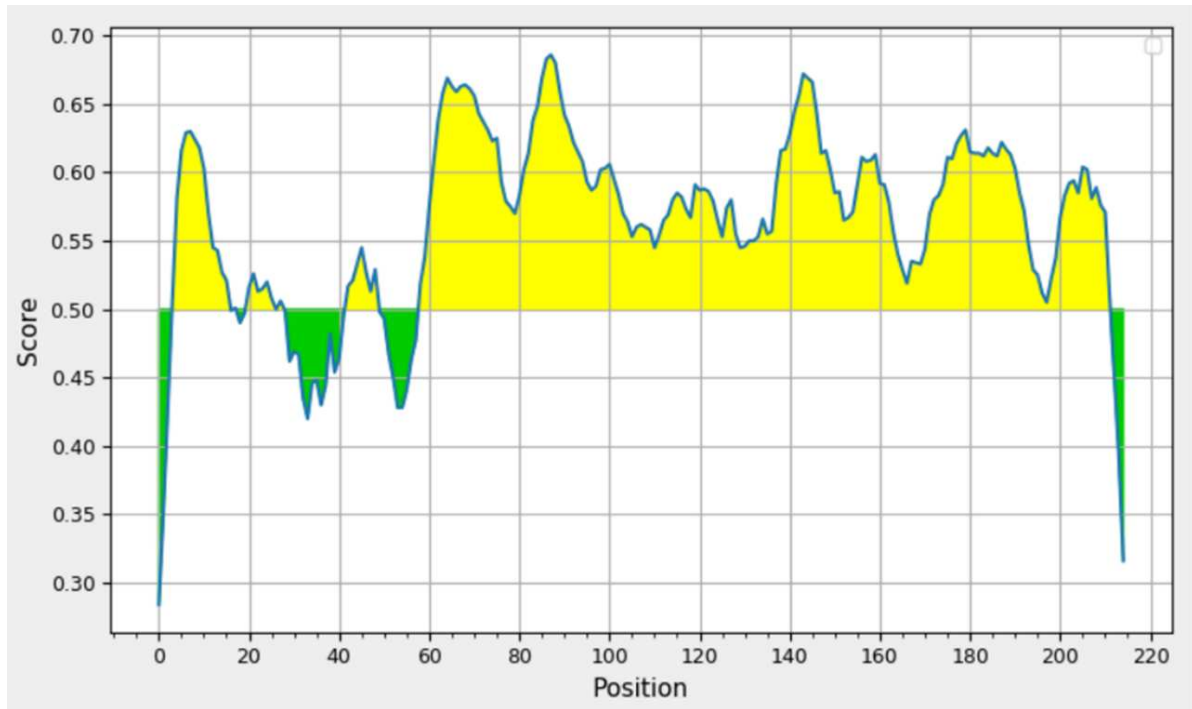


Figure 4. Antigenicity analysis of the L-HDAg protein sequence with the Bepipred program. The yellow peaks represent the part of the B-cell epitope and the green peaks represent non-B cell epitopes.

In Silico Analyse- L-HDAg modeling and alignment.

The trRosetta model for the L-HDAg structure covered all sequences it is possible to verify that the whole structure is completely compact and folded in helices (Fig. 5). The structural alignment between the AI and homology L-HDAg models revealed that the region of L-HDAg sequence between de amino acids GLY 12 and LYS 61 modeled in Phyre2 is very similar to the trRosetta structure, which possibly indicates a more conserved portion of these structures (Fig. 5). The 3D structure of the L-HDAg aligned with peptides HDAg1 and HDAg2 showed the epitopes selected are mimetic to immunogenic region protein of L-HDAg (Fig. 6).

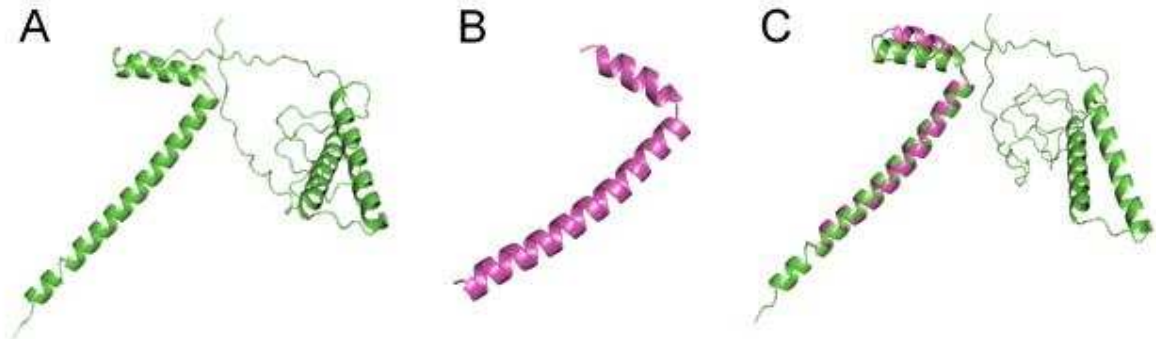


Figure 5. 3D structure of the L-HDAg (A) modeled by trRosetta (B) Modeled by Phyre 2 (C) Structural comparison between L-HDAg models from Phyre 2 (pink) and TrRosetta (green). The 3D-aligned region ranges from the amino acids GLY 12 to LYS 61.

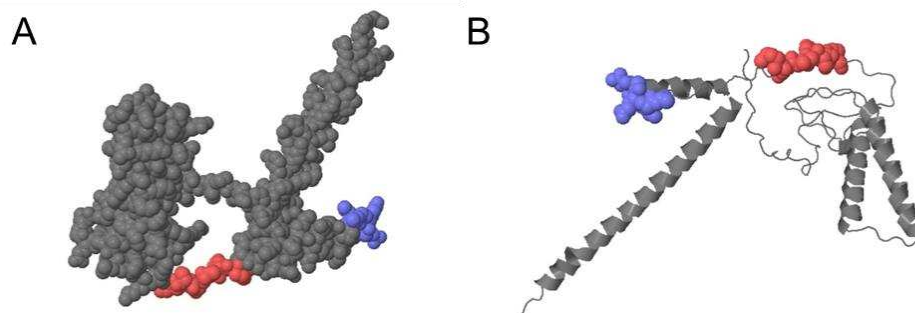


Figure 6. Alignments in 3D structures using the sequence of L-HDAg (gray) performed by PepSurf. Peptides were mapped in the L-HDAg; HDAG1 is represented in blue, and HDAG2 is represented in red (A) Space-fill model (B) Ribbon model.

Immunoreactivity of synthetic peptides and recombinant protein with serum

When comparing the reactivity by ELISA test of the three synthetic peptides (HDAG1, HDAG2, and HDAG3). We observed that the HDAG3 peptide had better reactivity. Therefore, the HDAG3 peptide was selected to be used in subsequent experiments. Two different serum concentrations (1:100, 1:250) and two HDAG3 concentrations (200 ng and 1 μ g) were evaluated

in 10 positive anti-HDV + serum samples and 10 HBV Control samples for test standardization (Fig. 7). The synthetic peptide HDAg3 demonstrated capability to differentiate pooled samples of serum from anti-HDV positive and hepatitis B patients.

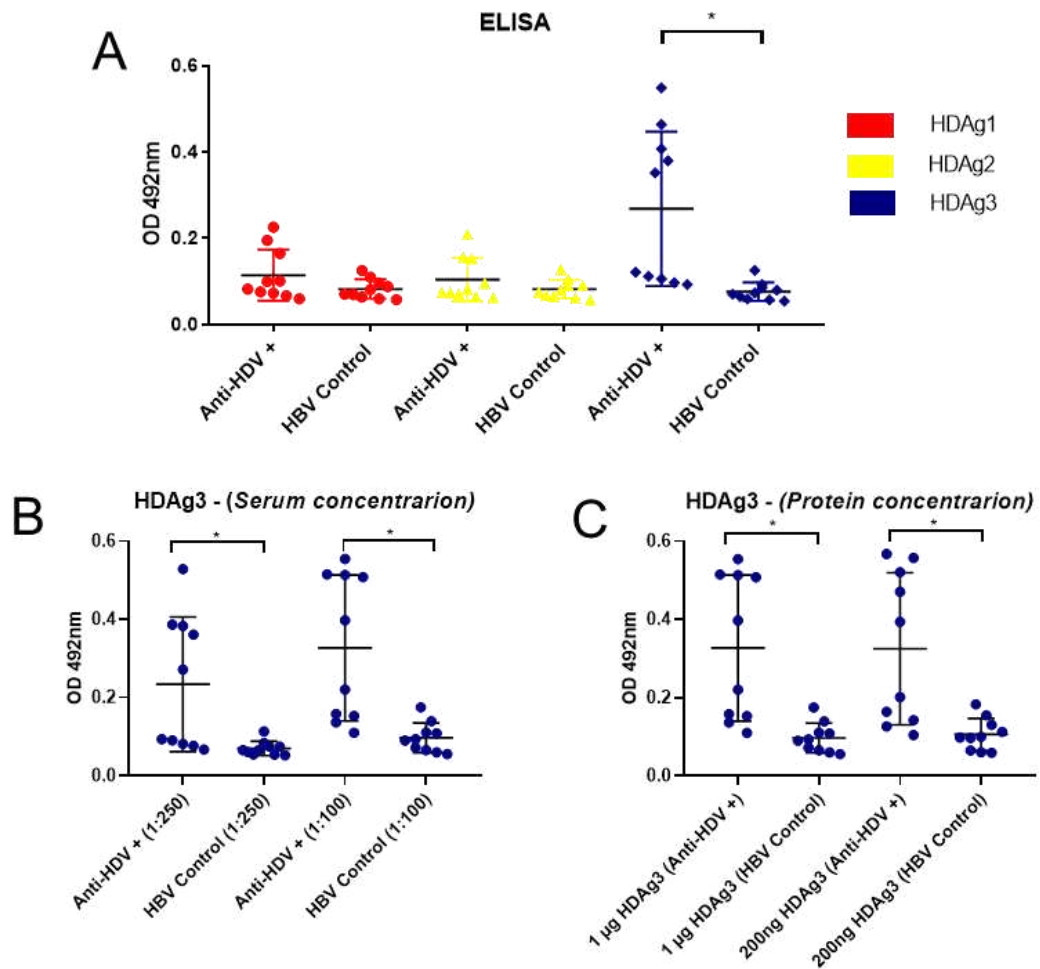


Figure 7. ELISA to evaluate the synthetic peptides. (A) Different synthetic peptides HDAg1, HDAg2, and HDAg3, (B) different concentrations of serum (1:100, 1:250) with HDAg3, and (C) different concentrations of HDAg3 (200 ng and 1 µg) of 10 serum anti-HDV+ from 10 serum HBV Control.

In this context, we selected the HDAg3 for additional analysis using an individual serum from 87 positive anti-HDV+ samples compared to 93 HBV Control samples presenting 81.72% of specificity, 57.47% of sensitivity, and AUC 0.717 (Fig. 8.A and 8.C). Subsequently, we assessed reactivity using an ELISA test based on the recombinant protein HDAgProt. The results demonstrated an increase in detection parameters presenting a sensitivity of 74.71%,

specificity of 97.85%, and AUC of 0.8906 when utilizing the same serum samples (Fig. 8.B and 8.D). This highlights the benefit of the use of recombinant protein HDAgProt.

A molecular assay to detect HDV RNA is used to evaluate active infection ³². In the intent to evaluate our recombinant protein HDAgProt with samples in active infection, we used 50 samples that obtained a positive result in HDV RT-qPCR compared to 93 HBV Control. The discrimination between hepatitis delta patients with HDV detection in RT-qPCR versus hepatitis B patients achieved an AUC of 0.9665, which yields a sensitivity of 88.0% when specificity is 98.92%, (Fig. 9). Additionally, we analyzed the genotype of these samples, resulting in the classification of 32 patients as genotype 3 (HDV-3) (Table 2).

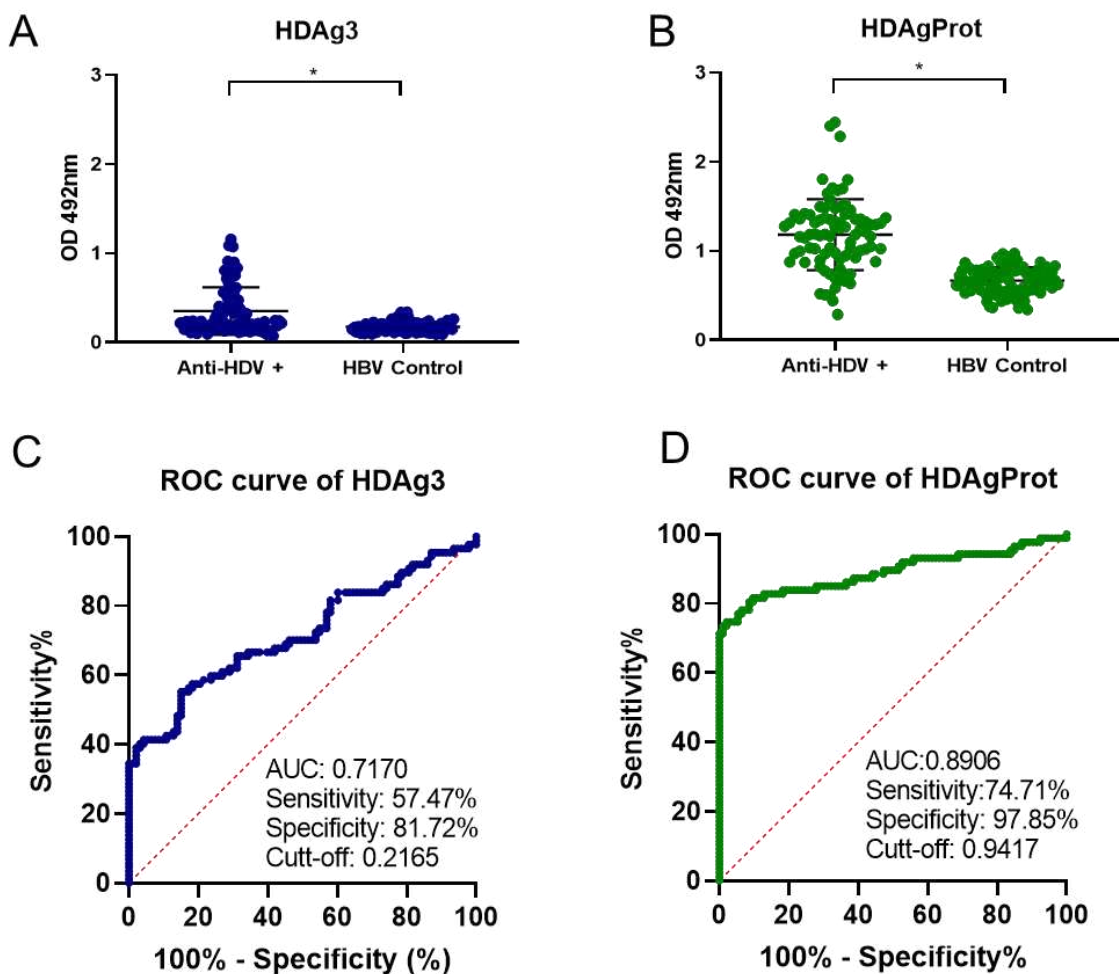


Figure 8. Reactivity of human serum samples based on HDAg3 and HDAgProt in ELISA, and respective, analysis of sensitivity, specificity, and AUC to compare anti-HDV+ and HBV Control. (A) reactivity using synthetic peptide HDAg3 (B) reactivity using recombinant protein HDAgProt, and the ROC curves for (C) HDAg3 and (D) HDAgProt.

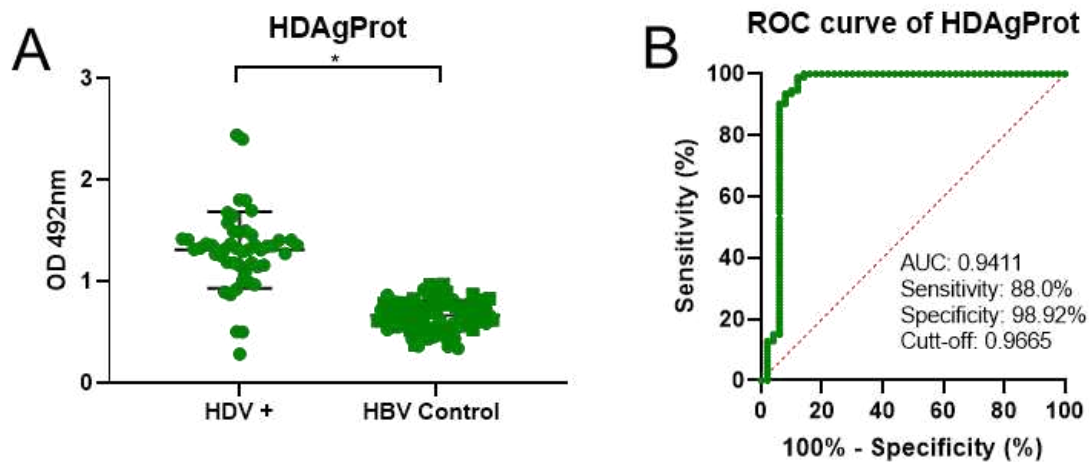


Figure 9. Reactivity of human serum samples based on HDAGProt and respective analysis of sensitivity, specificity, and AUC to compare hepatitis D (HDV +) patients with active infection and HBV Control. (A) Reactivity using recombinant protein HDAGProt and, respective, (B) ROC curves analysis.

ID sample	Viral Load (Log ₁₀ copies/mL)	Collection Date	Residence City	Genbank	HDV Genotype
4.3	6,02	14/08/2018	Cruzeiro do Sul – AC	OR792427	HDV-3
4.4	6,38	23/11/2018	Boca do Acre – AM	OR792428	HDV-3
4.9	3,69	29/10/2018	Guajará- AM	OR792429	HDV-3
4.18	4,69	12/06/2019	Rio Branco – AC	OR792430	HDV-3
4.20	6,50	22/02/2019	Rio Branco – AC	OR792431	HDV-3
4.23	5,36	28/01/2019	Rio Branco – AC	OR792432	HDV-3
4.27	6,52	19/12/2018	Rio Branco – AC	OR792433	HDV-3
4.31	5,27	11/10/2018	Rio Branco – AC	OR792434	HDV-3
4.38	5,04	26/07/2018	Rio Branco – AC	OR792435	HDV-3
4.39	7,72	11/07/2018	Rio Branco – AC	OR792436	HDV-3
4.48	5,05	13/04/2018	Rio Branco – AC	OR792437	HDV-3
4.52	6,37	16/12/2018	Rio Branco – AC	OR792438	HDV-3
4.54	6,40	19/12/2018	Porto Walter – AC	OR792439	HDV-3
4.56	4,46	08/01/2019	Cruzeiro do Sul – AC	OR792440	HDV-3
4.59	5,98	26/11/2018	Cruzeiro do Sul – AC	OR792441	HDV-3
4.71	5,99	31/10/2018	Cruzeiro do Sul – AC	OR792442	HDV-3
4.74	4,70	25/09/2018	Cruzeiro do Sul – AC	OR792443	HDV-3
4.76	7,68	31/08/2018	Tarauacá – AC	OR792444	HDV-3
4.77	6,10	31/08/2018	Envira – AM	OR792445	HDV-3
4.81	5,10	27/08/2018	Cruzeiro do Sul – AC	OR792446	HDV-3
4.82	6,17	21/08/2018	Sena Madureira – AC	OR792447	HDV-3
4.84	6,83	09/08/2018	Porto Walter – AC	OR792448	HDV-3

4.87	6,59	09/07/2018	Feijó – AC	OR792449	HDV-3
4.93	4,75	12/12/2018	Cruzeiro do Sul – AC	OR792450	HDV-3
4.94	6,33	03/08/2018	Sena Madureira – AC	OR792451	HDV-3
4.96	4,61	07/11/2018	Cruzeiro do Sul – AC	OR792452	HDV-3
4.98	5,93	06/11/2018	Porto Walter – AC	OR792453	HDV-3
4.105	5,62	05/07/2018	Rio Branco – AC	OR792454	HDV-3

Table 2. Genotype of HDV sample, epidemiological data, and viral load of HDV.

Discussion

A novel immunodiagnostic platform for hepatitis D detection based on novel HDV antigenic epitopes selected by *Phage Display* that recognize anti-HDV antibodies has the potential to make a significant impact on the detection rate of hepatitis D, enabling early diagnosis, timely initiation of treatment, and improving quality of life. It also can be critical for reducing the costs of hepatitis D diagnostics in both public and private healthcare services globally. From a translational perspective, this novel immunodiagnostic platform for hepatitis D detection based on HDAgProt can be translated into the medical clinic as a triage approach. The efficiency of this novel recombinant protein HDAgProt in an active infection scenario achieved an impressive AUC of 0.9665, with a sensitivity of 88%, and an outstanding specificity of 98.92% based on 50 serum samples of active hepatitis delta compared with 93 samples from hepatitis B patients. This recombinant protein HDAgProt applied in an ELISA-based immunodiagnostic platform was also capable to achieve an AUC of 0.8906 with a sensitivity of 74.71% and specificity of 97.85% comparing 87 serum samples from hepatitis delta patients (anti-HDV positive) with 93 hepatitis B patients.

HDV infection is a neglected disease with a high prevalence in low- and middle-income countries (LMICs) ^{34,35}. In Brazil, the Amazon region exhibits a higher prevalence of hepatitis D, impacting mainly isolated riverside and indigenous populations³⁶. The limited availability of diagnostic tests for hepatitis D in LMICs contributes to the underestimation of disease prevalence and also impairs timely diagnosis, leading to delays in the onset of treatment^{18,37}.

The current study employed *Phage Display* technology to establish a screening platform based on HDV mimetic molecules that interact with anti-HDV antibodies for application in HDV immunodiagnostic platforms. The screening of phages by reactivity in the Phage-ELISA assay was used to select best-performing clones to differentiate hepatitis delta patients (anti-HDV positive) from hepatitis B patients (Fig. 2). The phage-ELISA was used for a similar aim to develop a novel diagnostic platform for *visceral leishmaniasis* (VL) in human serum³⁸. In the present study, we performed phage-ELISA in pooled samples and also validated this novel HDAg3 synthetic peptide and recombinant protein based on selected phage sequences.

The sequences of peptide phages were aligned with L-HDAg using the Clustal Omega alignment tool (Fig. 3). The L-HDAg protein has been used as a target for diagnosis in other studies. In this context, an HDV lateral flow test for detecting anti-HDV antibodies used a recombinant L-HDAg with 25 kDa His-tagged protein in serum and plasma³⁹. Another serology assay to detect IgG anti-HDV with the ARCHITECT immunoassay instrument (Abbott Diagnostics, Abbott Park, IL) was tested in 15 samples from RNA HDV positive samples using a peptide from overlapping region of L-HDAg (aa 64–85) detecting 14 of 15 samples⁴⁰.

Bearing in mind that L-HDAg is an immunogenic protein that induces oxidative stress, and activates NF- κ B and STAT-3, leading to a dysregulation of inflammation, apoptosis, and invasion of the immune system⁴¹. The selected sequence of L-HDAg used in the present study was an epitope region (the part of the antigen that binds to the antibody) (Fig.4)²⁸ identified by Bepipred - Linear Epitope prediction 2.0. The 3D structure L-HDAg was not available in the RCSB Protein Data Bank. The present study was also a pioneer in modeling L-HDAg protein using TrRosetta and Phyre 2 programs. As depicted in Figure 6, it was shown that the synthetic peptides were overlapping in the epitope region of L-HDAg such on Linear Epitope prediction 2.0 analysis. This amino acid region (63-85) of L-HDAg protein was previously validated as an

immunogenic portion^{40,42,43}, this confirms the potential of HDAgProt as a molecule applied in diagnostics platforms of hepatitis Delta.

The reactivity of the peptides HDAg1, HDAg2, and HDAg3 was evaluated in ELISA and the HDAg3 was effective to perform differential detection of serum samples from hepatitis Delta patients (anti-HDV+) from hepatitis B patients. In this large-scale study, the HDAg3-based platform was validated with 87 hepatitis Delta patients (anti-HDV+) compared to 93 hepatitis B patients achieving a specificity of 81.72%, and sensitivity of 57.47% with an AUC of 0.7170. The HDAg3 sequence was used to construct a recombinant protein HDAgProt with additional modifications. Subsequently, an ELISA was conducted comparing samples from hepatitis Delta patients (anti-HDV+) with hepatitis B patients, resulting in a sensitivity of 74.71% and a high specificity of 97.85% with an AUC of 0.8906 (Fig.8); suggesting the potential application of the recombinant protein in a clinical screening test for controlling the spread of the disease.

Anti-HDV tests are also indicative of the patient's exposure to the virus in immunocompetent people⁴⁴, the hallmark of active HDV infection is RNA detection by molecular biology. When we evaluated only samples that were HDV RNA positive, the HDAgProt protein-based ELISA assay achieved a sensitivity of 88.0%, specificity of 98.92%, and AUC of 0.9665 testing on 50 serum samples of active hepatitis delta compared with 93 samples from hepatitis B patients (Fig. 9). Our test demonstrates efficacy in screening patients with active HDV infection.

In the genotypic analysis of our samples, all presented genotype 3 (Table 2), which is predominantly found in South America, notably in the western Amazon basin, and is associated with the most severe liver disease^{45,46}. The evaluation of another genotype must be further investigated for application in an immunoenzymatic platform for hepatitis delta detection.

Conclusion

Here, we showed the HDV mimetic molecule which interacts with anti-HDV antibodies based on *Phage Display* technology is a promising alternative for HDV detection using an immunoenzymatic platform. Our innovative diagnostic approach based on HDAgProt recombinant protein has the potential to significantly improve the detection rate of hepatitis Delta, allowing for early diagnosis and timely initiation of treatment, thereby improving overall quality of life. Notably, this breakthrough can reduce economic costs associated with hepatitis Delta diagnostics in healthcare services globally. It is particularly critical in the Amazon region and in low- and middle-income countries, where the prevalence of the hepatitis Delta remains underestimated due to limited diagnostic availability. Highlighting the potential use in another's efficient, fast, portable, and low-cost platforms for HDV detection.

ADDITIONAL INFORMATION

Competing financial interests

The authors declare no competing financial interests.

Authors' contributions

M.A.C., L.R.G[†], F.A.A., R.S-S, I.M.S.L, conceptualization; M.A.C., R.S.M.P., R.B.S. sample acquisition; M.A.C., F.A.A.S., R.C.S., T.P.R., A.A.S.O., B.S.A., L.F.A.S., R.B.S., I.P.S., M.G-V., D.C.C., I.M.S.L., M.M.M performed the experiments; M.AC., R.C.S., T.P.R., A.A.S.O., B.S.A., L.F.A.S., R.B.S., R.S.M.P., I.P.S., M.G-V., D.C.C., I.M.S.L., A.M.P-S., A.D.R., M.M.M., D.A.M., D.V., R.S-S., F.A.A.S., analyzed the data; D.V., L.R.G., R. S-S., resource; M.A.C., R.C.S., T.P.R., A.A.S.O., L.F.A.S., R.B.S., R.S.M.P., I.P.S., M.G-V., D.C.C., I.M.S.L., A.M.P-S., A.D.R., M.M.M., D.A.M., D.V., R. S-S., F.A.A.S. wrote the paper

Acknowledgments

Professor Dr. Luiz Ricardo Goulart who led the beginning of the work, gratitude and honor for guiding me firsts step in this research.

Greiciele Carvalho Leite, Janaína Mazaro, Janete Taynã Nascimento Rodrigues, Camilo Matheus Monteiro Braga de Oliveira, Francilene de Oliveira Braz, Carmen Silva dos Santos Silva, they support the research at Central Laboratory of Public Health of Acre, Secretary of Health of Acre, Acre, Brazil.

REFERENCES

1. Walker, P. J. *et al.* Changes to virus taxonomy and to the International Code of Virus Classification and Nomenclature ratified by the International Committee on Taxonomy of Viruses (2021). *Arch Virol* **166**, 2633–2648 (2021).
2. Caviglia, G. P., Ciancio, A. & Rizzetto, M. A Review of HDV Infection. *Viruses* **14**, (2022).
3. Da, B. L., Heller, T. & Koh, C. Hepatitis D infection: from initial discovery to current investigational therapies. *Gastroenterology Report* **7**, 231–245 (2019).
4. Netter, H. J., Barrios, M. H., Littlejohn, M. & Yuen, L. K. W. Hepatitis Delta Virus (HDV) and Delta-Like Agents: Insights Into Their Origin. *Front Microbiol* **12**, 652962 (2021).
5. Botelho-Souza, L. F., Vasconcelos, M. P. A., dos Santos, A. de O., Salcedo, J. M. V. & Vieira, D. S. Hepatitis delta: virological and clinical aspects. *Virol J* **14**, 177 (2017).
6. Cunha, C., Tavanez, J. P. & Gudima, S. Hepatitis delta virus: A fascinating and neglected pathogen. *WJV* **4**, 313 (2015).
7. Le Gal, F. *et al.* Genetic diversity and worldwide distribution of the deltavirus genus: A study of 2,152 clinical strains. *Hepatology* **66**, 1826–1841 (2017).

8. Chen, H.-Y. *et al.* Prevalence and burden of hepatitis D virus infection in the global population: a systematic review and meta-analysis. *Gut* **68**, 512–521 (2019).
9. Stockdale, A. J. *et al.* The global prevalence of hepatitis D virus infection: Systematic review and meta-analysis. *J Hepatol* **73**, 523–532 (2020).
10. Miao, Z. *et al.* Estimating the Global Prevalence, Disease Progression, and Clinical Outcome of Hepatitis Delta Virus Infection. *J Infect Dis* **221**, 1677–1687 (2020).
11. Organization, W. H. Hepatitis D. <https://www.who.int/news-room/fact-sheets/detail/hepatitis-d> (2023).
12. Koh, C., Heller, T. & Glenn, J. S. Pathogenesis of and New Therapies for Hepatitis D. *Gastroenterology* **156**, 461-476.e1 (2019).
13. Turon-Lagot, V., Saviano, A., Schuster, C., Baumert, T. F. & Verrier, E. R. Targeting the Host for New Therapeutic Perspectives in Hepatitis D. *J Clin Med* **9**, (2020).
14. Tseligka, E. D., Clément, S. & Negro, F. HDV Pathogenesis: Unravelling Ariadne's Thread. *Viruses* **13**, (2021).
15. Kamal, H. & Aleman, S. Natural history of untreated HDV patients: always a progressive disease? **32**.
16. Farci, P. & Niro, G. Clinical Features of Hepatitis D. *Semin Liver Dis* **32**, 228–236 (2012).
17. Niro, G. A., Ferro, A., Cicerchia, F., Brascugli, I. & Durazzo, M. Hepatitis delta virus: From infection to new therapeutic strategies. *World J Gastroenterol* **27**, 3530–3542 (2021).
18. Ceesay, A. *et al.* Viral Diagnosis of Hepatitis B and Delta: What We Know and What Is Still Required? Specific Focus on Low- and Middle-Income Countries. *Microorganisms* **10**, 2096 (2022).

19. Hughes, S. A., Wedemeyer, H. & Harrison, P. M. Hepatitis delta virus. *The Lancet* **378**, 73–85 (2011).
20. Ahn, J. & Gish, R. G. Hepatitis D Virus: A Call to Screening. *Hepatology* **58**, 8 (2014).
21. Papatheodoridi, M. & Papatheodoridis, G. V. Is hepatitis delta underestimated? *Liver Int* **41 Suppl 1**, 38–44 (2021).
22. Ledsgaard, L. *et al.* Advances in antibody phage display technology. *Drug Discovery Today* **27**, 2151–2169 (2022).
23. Barbas, C. F., Burton, D. R. & Silverman, G. J. *Phage Display: A Laboratory Manual*. (Cold Spring Harbor Laboratory Press, 2001).
24. Pande, J., Szewczyk, M. M. & Grover, A. K. Phage display: Concept, innovations, applications and future. *Biotechnology Advances* **28**, 849–858 (2010).
25. Smith, G. P. Phage Display: Simple Evolution in a Petri Dish (Nobel Lecture). *Angewandte Chemie International Edition* **58**, 14428–14437 (2019).
26. de Souza, T. A. *et al.* Eosinophilic esophagitis auxiliary diagnosis based on a peptide ligand to eosinophil cationic protein in esophageal mucus of pediatric patients. *Sci Rep* **12**, 12226 (2022).
27. Sievers, F. *et al.* Fast, scalable generation of high-quality protein multiple sequence alignments using Clustal Omega. *Molecular Systems Biology* **7**, 539 (2011).
28. BepiPred-2.0: improving sequence-based B-cell epitope prediction using conformational epitopes | Nucleic Acids Research | Oxford Academic.
<https://academic.oup.com/nar/article/45/W1/W24/3787843>.
29. T, D. *et al.* Structural immunoinformatics approach for rational design of a multi-epitope vaccine against triple negative breast cancer. *International Journal of Biological Macromolecules* **243**, 125209 (2023).

30. Du, Z. *et al.* The trRosetta server for fast and accurate protein structure prediction. *Nat Protoc* **16**, 5634–5651 (2021).
31. Zuccola, H. J., Rozzelle, J. E., Lemon, S. M., Erickson, B. W. & Hogle, J. M. Structural basis of the oligomerization of hepatitis delta antigen. *Structure* **6**, 821–830 (1998).
32. Da Silva Queiroz, J. A. *et al.* Development of quantitative multiplex RT-qPCR one step assay for detection of hepatitis delta virus. *Sci Rep* **13**, 12073 (2023).
33. Casey, J. L., Brown, T. L., Colan, E. J., Wignall, F. S. & Gerin, J. L. A genotype of hepatitis D virus that occurs in northern South America. *Proc. Natl. Acad. Sci. U.S.A.* **90**, 9016–9020 (1993).
34. Gill, U. S. The immune landscape in hepatitis delta virus infection—Still an open field. *Journal of Viral Hepatitis* **30**, 22–26 (2023).
35. Tharwani, A. & Hamid, S. Elimination of HDV: Epidemiologic implications and public health perspectives. *Liver International* **43**, 101–107 (2023).
36. Cabezas, C. & Braga, W. Hepatitis B Virus and Delta Infection: Special Considerations in the Indigenous and Isolated Riverside Populations in the Amazon Region. *Clin Liver Dis (Hoboken)* **16**, 117–122 (2020).
37. Chen, L.-Y., Pang, X.-Y., Goyal, H., Yang, R.-X. & Xu, H.-G. Hepatitis D: challenges in the estimation of true prevalence and laboratory diagnosis. *Gut Pathog* **13**, 66 (2021).
38. Salles, B. C. S. *et al.* Leishmania infantum mimotopes and a phage–ELISA assay as tools for a sensitive and specific serodiagnosis of human visceral leishmaniasis. *Diagnostic Microbiology and Infectious Disease* **87**, 219–225 (2017).
39. Lempp, F. A. *et al.* A Rapid Point-of-Care Test for the Serodiagnosis of Hepatitis Delta Virus Infection. *Viruses* **13**, (2021).
40. Coller, K. E. *et al.* Development and performance of prototype serologic and molecular tests for hepatitis delta infection. *Sci Rep* **8**, 2095 (2018).

41. Oberhardt, V., Hofmann, M., Thimme, R. & Neumann-Haefelin, C. Adaptive Immune Responses, Immune Escape and Immune-Mediated Pathogenesis during HDV Infection. *Viruses* **14**, (2022).
42. Villiers, M.-B. *et al.* Protein-Peptide Arrays for Detection of Specific Anti-Hepatitis D Virus (HDV) Genotype 1, 6, and 8 Antibodies among HDV-Infected Patients by Surface Plasmon Resonance Imaging. *J Clin Microbiol* **53**, 1164–1171 (2015).
43. Wang, J. G., Jansen, R. W., Brown, E. A. & Lemon, S. M. Immunogenic domains of hepatitis delta virus antigen: peptide mapping of epitopes recognized by human and woodchuck antibodies. *J Virol* **64**, 1108–1116 (1990).
44. Asselah, T. & Rizzetto, M. Hepatitis D Virus Infection. *N Engl J Med* **389**, 58–70 (2023).
45. Gomes-Gouvêa, M. S. *et al.* Hepatitis B virus and hepatitis delta virus genotypes in outbreaks of fulminant hepatitis (Labrea black fever) in the western Brazilian Amazon region. *J Gen Virol* **90**, 2638–2643 (2009).
46. Lange, M., Zaret, D. & Kushner, T. Hepatitis Delta: Current Knowledge and Future Directions. *Gastroenterol Hepatol (N Y)* **18**, 508–520 (2022).

3 CONCLUSÕES

Capítulo I

Foi aplicado métodos multivariados para análise dos espectros de ATR-FTIR em uma grande coorte de sujeitos provenientes da Amazônia Brasileira, o método de suporte de vetores de máquinas foi o que melhor distinguiu os sujeitos controles e pacientes com hepatite B.

Capítulo II

Foi desenvolvido moléculas miméticas ao HDV por *Phage Display* que reconhecem anticorpos Anti-HDV. A proteína recombinante HDAgProt conseguiu distinguir de forma eficiente os pacientes mono-infectados com hepatite B dos pacientes com hepatite Delta aplicado em uma plataforma imunoenzimáticas.

REFERÊNCIAS

- AGÊNCIA NACIONAL DE VIGILÂNCIA SANITÁRIA (Brasil). **Consultas**. Local: Brasília, DF, 2023. Disponível em: <<https://consultas.anvisa.gov.br/#/saude/q/?nomeTecnico=hdv>>. Acesso em: 11 nov. 2023.
- ALI, Salmann *et al.* ATR-FTIR spectroscopy-based differentiation of hepatitis C and dengue infection in human freeze-dried sera. **Infrared Physics & Technology**, [s. l.], v. 118, p. 1-4, 2021. DOI: <https://doi.org/10.1016/j.infrared.2021.103912>. Acesso em: 03 nov. 2023.
- ALI, Salmann; NASEER, Khulla; QAZI, Javaria. Diagnosis of HCV infection using attenuated total Reflection-FTIR spectra of Freeze-Dried sera. **Infrared Physics & Technology**, [s. l.], v. 121, p. 1-7, 2022. DOI: <https://doi.org/10.1016/j.infrared.2021.104019>. Acesso em: 03 nov. 2023.
- AREAL, Alan Hudson Ganum. Estudo clínico-epidemiológico da Hepatite Delta no município de Sena Madureira – Acre – Brasil. 2015. 130 f., il. Dissertação (Mestrado em Medicina Tropical) – Universidade de Brasília, Brasília, 2015. DOI: <http://dx.doi.org/10.26512/2015.08.D.23493>. Acesso em: 11 nov 2023.
- ASSELAH, Tarik; RIZZETTO, Mario. Hepatitis D Virus Infection. **New England Journal of Medicine**, [s. l.], v. 389, n. 1, p. 58–70, 2023. DOI: <https://doi.org/10.1056/NEJMra2212151>. Acesso em: 03 nov. 2023.
- BAKER, Matthew J *et al.* Using Fourier transform IR spectroscopy to analyze biological materials. **Nature Protocols**, [s. l.], v. 9, n. 8, p. 1771–1791, 2014. DOI: <https://doi.org/10.1038/nprot.2014.110>. Acesso em: 03 nov. 2023.
- BENSABATH, G. et al. Hepatitis delta virus infection and Labrea hepatitis. Prevalence and role in fulminant hepatitis in the Amazon Basin. **JAMA**, [s. l.], v. 258, n. 4, p. 479–483, 1987. DOI: <https://doi.org/10.1001/jama.1987.03400040077025>. Acesso em: 03 nov. 2023.
- BOTELHO-SOUZA, Luan Felipe *et al.* Development of a reverse transcription quantitative real-time PCR-based system for rapid detection and quantitation of hepatitis delta virus in the western Amazon region of Brazil. **Journal of Virological Methods**, [s. l.], v. 197, p. 19–24, 2014. DOI: <https://doi.org/10.1016/j.jviromet.2013.11.016>. Acesso em: 03 nov. 2023.
- BOTELHO-SOUZA, Luan Felipe *et al.* Hepatitis delta: virological and clinical aspects. **Virology Journal**, [s. l.], v. 14, n. 1, p. 1-15, 2017. DOI: <https://doi.org/10.1186/s12985-017-0845-y>. Acesso em: 03 nov. 2023.
- BRASIL. Ministério da Saúde, **Manual técnico para o diagnóstico das hepatites virais**. 2.ed. Brasília, DF, 2018. Disponível em: <http://antigo.aids.gov.br/pt-br/noticias/manual-tecnico-para-o-diagnostico-das-hepatites-virais-e-atualizado>. Acesso em: 11 nov. 2023.
- BRASIL. Ministério da Saúde. **Boletim Epidemiológico - Hepatites Virais 2023**. Brasília, DF, 2023. Disponível em: https://www.gov.br/aids/pt-br/central-de-conteudo/boletins-epidemiologicos/2023/hepatites-virais/boletim-epidemiologico-hepatites-virais-_2023.pdf/view. ISSN: 9352-7864. Acesso em: 13 dez.2023.a

BRASIL. Ministério da Saúde. **Hepatite D**. Brasília, DF: MS, 2023. Portal. Disponível em: <https://www.gov.br/saude/pt-br/assuntos/saude-de-a-a-z/h/hepatites-virais/hepatite-d#:~:text=Outras%20medidas%20envolvem%3A%20uso%20de,tatuagem%20e%20coloca%C3%A7%C3%A3o%20de%20piercings>. Acesso em: 14 dez. 2023. b

BRASIL. Ministério da Saúde, **Protocolo Clínico e Diretrizes Terapêuticas de Hepatite B e Confeções**. 1. ed. Brasília, DF, 2023. Disponível em: https://bvsm.s.saude.gov.br/bvs/publicacoes/protocolo_clinico_diretrizes_terapeuticas_hepbdigital.pdf. Acesso em: 11 nov. 2023. c

CABEZAS, Sheila *et al.* Selection of phage-displayed human antibody fragments on Dengue virus particles captured by a monoclonal antibody: Application to the four serotypes. **Journal of Virological Methods**, [s. l.], v. 147, n. 2, p. 235–243, 2008. DOI: <https://doi.org/10.1016/j.jviromet.2007.09.001>. Acesso em: 03 nov. 2023.

CAIXETA, Douglas C. *et al.* Salivary molecular spectroscopy: A sustainable, rapid and non-invasive monitoring tool for diabetes mellitus during insulin treatment. **PLOS ONE**, [s. l.], v. 15, n. 3, p. 1-18, 2020. DOI: <https://doi.org/10.1371/journal.pone.0223461>. Acesso em: 03 nov. 2023.

CASEY, J.L. *et al.* Peptide mimics selected from immune sera using phage display technology can replace native antigens in the diagnosis of Epstein–Barr virus infection. **Protein Engineering, Design and Selection**, [s. l.], v. 22, n. 2, p. 85–91, 2009. DOI: <https://doi.org/10.1093/protein/gzn076>. Acesso em: 03 nov. 2023.

CHEN, Lin-Yuan *et al.* Hepatitis D: challenges in the estimation of true prevalence and laboratory diagnosis. **Gut pathogens**, [s. l.], v. 13, n. 1, p. 1-9, 2021. DOI: <https://doi.org/10.1186/s13099-021-00462-0>. Acesso em: 03 nov. 2023.

CHOU, Huei-Chi *et al.* Hepatitis Delta Antigen Mediates the Nuclear Import of Hepatitis Delta Virus RNA. **Journal of Virology**, [s. l.], v. 72, n. 5, p. 3684–3690, 1998. DOI: <https://doi.org/10.1128/JVI.72.5.3684-3690.1998>. Acesso em: 03 nov. 2023.

CUNHA, Celso; TAVANEZ, João Paulo; GUDIMA, Severin. Hepatitis delta virus: A fascinating and neglected pathogen. **World Journal of Virology**, [s. l.], v. 4, n. 4, p. 313-322, 2015. DOI: <https://doi.org/10.5501/wjv.v4.i4.313>. Acesso em: 03 nov. 2023.

DA, Ben L; HELLER, Theo; KOH, Christopher. Hepatitis D infection: from initial discovery to current investigational therapies. **Gastroenterology Report**, [s. l.], v. 7, n. 4, p. 231–245, 2019. DOI: <https://doi.org/10.1093/gastro/goz023>. Acesso em: 03 nov. 2023..

DANTAS, Thor. **Aspectos Epidemiológicos da infecção pelo vírus da C e coinfeções com o vírus da hepatite B e Delta no estado do Acre, Amazônia Ocidental, Brasileira**. 2010.145f.. Tese (Doutorado em Medicina Tropical) - Universidade de Brasília, Brasília, DF, 2010. Disponível em: <http://repositorio.unb.br/jspui/handle/10482/8157>. Acesso em: 08 dez. 2023.

QUEIROZ, Jackson Alves Silva *et al.* Development of quantitative multiplex RT-qPCR one step assay for detection of hepatitis delta virus. **Scientific Reports**, [s. l.], v. 13, n. 1, p. 1-8, 2023. DOI: <https://doi.org/10.1038/s41598-023-37756-z>. Acesso em: 03 nov. 2023.

- DU, Taofeng *et al.* Biotinylated Single-Domain Antibody-Based Blocking ELISA for Detection of Antibodies Against Swine Influenza Virus. **International Journal of Nanomedicine**, [s. l.], v. 14, p. 9337–9349, 2019. DOI: <https://doi.org/10.2147/IJN.S218458>. Acesso em: 03 nov. 2023.
- EBRAHIMIZADEH, Walead; RAJABIBAZL, Masoumeh. Bacteriophage Vehicles for Phage Display: Biology, Mechanism, and Application. **Current Microbiology**, [s. l.], v. 69, n. 2, p. 109–120, 2014. DOI: <https://doi.org/10.1007/s00284-014-0557-0>. Acesso em: 03 nov. 2023.
- FADLELMOULA, Ahmed *et al.* Fourier Transform Infrared (FTIR) Spectroscopy to Analyse Human Blood over the Last 20 Years: A Review towards Lab-on-a-Chip Devices. **Micromachines**, [s. l.], v. 13, n. 2, p. 1-20, 2022. DOI: <https://doi.org/10.3390/mi13020187>. Acesso em: 03 nov. 2023.
- FADLELMOULA, A. *et al.* A Review of Machine Learning Methods Recently Applied to FTIR Spectroscopy Data for the Analysis of Human Blood Cells. **Micromachines**, [s. l.], v. 14, n. 6, p. 1145–1145, 2023. DOI: <http://doi.org/10.3390/mi14061145>. Acesso em: 26 nov. 2023.
- FARCI, Patrizia; NIRO, Grazia. Clinical Features of Hepatitis D. **Seminars in Liver Disease**, [s. l.], v. 32, n. 03, p. 228–236, 2012. DOI: <http://dx.doi.org/10.1055/s-0032-1323628>. Acesso em: 13 dez. 2023.
- FONSECA, José Carlos Ferraz da. Hepatite D. **Revista da Sociedade Brasileira de Medicina Tropical**, [s. l.], v. 35, n. 2, p. 181–190, 2002. DOI: <https://doi.org/10.1590/S0037-86822002000200009>. Acesso em: 03 nov. 2023.
- FONSECA, José Carlos Ferraz da *et al.* Hepatite fulminante e febre negra de Lábrea: estudo de 5 casos procedentes de Codajás, Amazonas, Brasil. **Revista da Sociedade Brasileira de Medicina Tropical**, [s. l.], v. 16, p. 144–147, 1983. DOI: <https://doi.org/10.1590/S0037-86821983000300004>. Acesso em: 03 nov. 2023.
- GRECO-STEWART, Valerie S. *et al.* The human RNA polymerase II interacts with the terminal stem-loop regions of the hepatitis delta virus RNA genome. **Virology**, [s. l.], v. 357, n. 1, p. 68–78, 2007. DOI: <https://doi.org/10.1016/j.virol.2006.08.010>. Acesso em: 03 nov. 2023.
- GRECO-STEWART, Valerie S.; SCHISSEL, Erica; PELCHAT, Martin. The hepatitis delta virus RNA genome interacts with the human RNA polymerases I and III. **Virology**, [s. l.], v. 386, n. 1, p. 12–15, 2009. DOI: <https://doi.org/10.1016/j.virol.2009.02.007>. Acesso em: 03 nov. 2023.
- HAMZEH-MIVEHROUD, Maryam *et al.* Phage display as a technology delivering on the promise of peptide drug discovery. **Drug Discovery Today**, [s. l.], v. 18, n. 23, p. 1144–1157, 2013. DOI: <https://doi.org/10.1016/j.drudis.2013.09.001>. Acesso em: 03 nov. 2023.
- HERRSCHER, Charline; ROINGEARD, Philippe; BLANCHARD, Emmanuelle. Hepatitis B Virus Entry into Cells. **Cells**, [s. l.], v. 9, n. 6, p.1-15, 2020. DOI: <https://doi.org/10.3390/cells9061486>. Acesso em: 03 nov. 2023.

HEUSCHKEL, Margaux J.; BAUMERT, Thomas F.; VERRIER, Eloi R. Cell Culture Models for the Study of Hepatitis D Virus Entry and Infection. **Viruses**, [s. l.], v. 13, n. 8, p. 1-10 2021. DOI: <https://doi.org/10.3390/v13081532>. Acesso em: 03 nov. 2023.

HUGHES, Sarah A; WEDEMEYER, Heiner; HARRISON, Phillip M. Hepatitis delta virus. **The Lancet**, [s. l.], v. 378, n. 9785, p. 73–85, 2011. DOI: [https://doi.org/10.1016/S0140-6736\(10\)61931-9](https://doi.org/10.1016/S0140-6736(10)61931-9). Acesso em: 03 nov. 2023.

JAROSZEWICZ, Weronika *et al.* Phage display and other peptide display technologies. **FEMS Microbiology Reviews**, [s. l.], v. 46, n. 2, p. 1-25, 2022. DOI: <https://doi.org/10.1093/femsre/fuab052>. Acesso em: 03 nov. 2023.

KIRSCH, Martina Inga *et al.* Development of human antibody fragments using antibody phage display for the detection and diagnosis of Venezuelan equine encephalitis virus (VEEV). **BMC Biotechnology**, [s. l.], v. 8, n. 1, p. 1-15, 2008. DOI: <https://doi.org/10.1186/1472-6750-8-66>. Acesso em: 03 nov. 2023.

KOFFAS, Apostolos; GILL, Upkar S. Hepatitis B and D: an overview of the diagnosis and management. *Medicine*, [s. l.], v. 51, n. 5, p. 351–355, 2023. DOI: <https://doi.org/10.1016/j.mpmed.2023.02.013>. Acesso em: 14 dez. 2023.

KOH, Christopher; DA, Ben L.; GLENN, Jeffrey S. HBV/HDV Coinfection: Emerging therapeutic options for a challenging disease. **Clinics in liver disease**, [s. l.], v. 23, n. 3, p. 557–572, 2019. DOI: <https://doi.org/10.1016/j.cld.2019.04.005>. Acesso em: 03 nov. 2023.

KOH, Christopher; HELLER, Theo; GLENN, Jeffrey S. Pathogenesis of and New Therapies for Hepatitis D. **Gastroenterology**, [s. l.], v. 156, n. 2, p. 461-476.e1, 2019. DOI: <https://doi.org/10.1053/j.gastro.2018.09.058>. Acesso em: 03 nov. 2023.

LARRALDE, Osmany G. *et al.* Identification of hepatitis A virus mimotopes by phage display, antigenicity and immunogenicity. **Journal of Virological Methods**, [s. l.], v. 140, n. 1, p. 49–58, 2007. DOI: <https://doi.org/10.1016/j.jviromet.2006.10.015>. Acesso em: 03 nov. 2023.

LI, Wei *et al.* Rapid identification of a human antibody with high prophylactic and therapeutic efficacy in three animal models of SARS-CoV-2 infection. **Proceedings of the National Academy of Sciences of the United States of America**, [s. l.], v. 117, n. 47, p. 29832–29838, 2020. DOI: <https://doi.org/10.1073/pnas.2010197117>. Acesso em: 03 nov. 2023.

LIU, Jinny L. *et al.* Selection and characterization of protective anti-chikungunya virus single domain antibodies. **Molecular Immunology**, [s. l.], v. 105, p. 190–197, 2019. DOI: <https://doi.org/10.1016/j.molimm.2018.11.016>. Acesso em: 03 nov. 2023.

LOPES, Jéssica *et al.* FTIR and Raman Spectroscopy Applied to Dementia Diagnosis Through Analysis of Biological Fluids. **Journal of Alzheimer's Disease**, [s. l.], v. 52, n. 3, p. 801–812, 2016. DOI: <https://doi.org/10.3233/JAD-151163>. Acesso em: 03 nov. 2023.

LUCIFORA, Julie; DELPHIN, Marion. Current knowledge on Hepatitis Delta Virus replication. **Antiviral research**, Netherlands, v. 179, p. 1-8, 2020. DOI: <https://doi.org/10.1016/j.antiviral.2020.104812>. Acesso em: 03 nov. 2023.

- MAGALHÃES, Sandra; GOODFELLOW, Brian J.; NUNES, Alexandra. FTIR spectroscopy in biomedical research: how to get the most out of its potential. **Applied Spectroscopy Reviews**, [s. l.], v. 56, n. 8–10, p. 869–907, 2021. DOI: <https://doi.org/10.1080/05704928.2021.1946822>. Acesso em: 03 nov. 2023.
- MENTHA, Nathalie *et al.* A review on hepatitis D: From virology to new therapies. **Journal of advanced research**, [s. l.], v. 17, p. 3–15, 2019. DOI: <https://doi.org/10.1016/j.jare.2019.03.009>. Acesso em: 03 nov. 2023.
- MWALE, Pharaoh Fellow *et al.* Expression, Purification, and Characterization of Anti-Zika virus Envelope Protein: Polyclonal and Chicken-Derived Single Chain Variable Fragment Antibodies. **International Journal of Molecular Sciences**, [s. l.], v. 21, n. 2, p. 1-21, 2020. DOI: <https://doi.org/10.3390/ijms21020492>. Acesso em: 03 nov. 2023.
- NASEER, Khulla; ALI, Salmann; QAZI, Javaria. ATR-FTIR spectroscopy as the future of diagnostics: a systematic review of the approach using bio-fluids. **Applied Spectroscopy Reviews**, [s. l.], v. 56, n. 2, p. 85–97, 2021. DOI: <https://doi.org/10.1080/05704928.2020.1738453>. Acesso em: 03 nov. 2023.
- OLIVEIRA, Marcelo Siqueira de *et al.* Evidências científicas sobre a hepatite Delta no Brasil: revisão integrativa da literatura. **Acta Paulista de Enfermagem**, [s. l.], v. 30, n. 6, p. 658–666, 2017. DOI: <https://doi.org/10.1590/1982-0194201700091>. Acesso em: 03 nov. 2023.
- PANDE, Jyoti; SZEWCZYK, Magdalena M.; GROVER, Ashok K. Phage display: Concept, innovations, applications and future. **Biotechnology Advances**, [s. l.], v. 28, n. 6, p. 849–858, 2010. DOI: <https://doi.org/10.1016/j.biotechadv.2010.07.004>. Acesso em: 03 nov. 2023.
- PEREBOEVA, L. A. *et al.* Hepatitis C epitopes from phage-displayed cDNA libraries and improved diagnosis with a chimeric antigen. **Journal of Medical Virology**, [s. l.], v. 60, n. 2, p. 144–151, 2000. DOI: [https://doi.org/10.1002/\(SICI\)1096-9071\(200002\)60:2144::AID-JMV73.0.CO;2-G](https://doi.org/10.1002/(SICI)1096-9071(200002)60:2144::AID-JMV73.0.CO;2-G). Acesso em: 03 nov. 2023.
- PEREZ-VARGAS, Jimena *et al.* Enveloped viruses distinct from HBV induce dissemination of hepatitis D virus in vivo. **Nature communications**, [s. l.], v. 10, n. 1, p. 1-15, 2019. DOI: <https://doi.org/10.1038/s41467-019-10117-z>. Acesso em: 03 nov. 2023.
- PIERRE, Khalfi *et al.* Hepatitis D virus: Improving virological knowledge to develop new treatments. **Antiviral Research**, [s. l.], p. 1-15, 2022. DOI: <https://doi.org/10.1016/j.antiviral.2022.105461> . Acesso em: 03 nov. 2023.
- RIZZETTO, M. *et al.* Transmission of the Hepatitis B Virus-Associated Delta Antigen to Chimpanzees. **The Journal of Infectious Diseases**, [s. l.], v. 141, n. 5, p. 590–602, 1980. DOI: <https://doi.org/10.1093/infdis/141.5.590> . Acesso em: 03 nov. 2023.a
- RIZZETTO, M *et al.* delta Agent: association of delta antigen with hepatitis B surface antigen and RNA in serum of delta-infected chimpanzees. **Proceedings of the National Academy of Sciences of the United States of America**, [s. l.], v. 77, n. 10, p. 6124–6128, 1980. DOI: <https://doi.org/10.1073/pnas.77.10.6124> Acesso em: 03 nov. 2023.b
- RIZZETTO, Mario. Hepatitis D Virus: Introduction and Epidemiology. **Cold Spring Harbor Perspectives in Medicine**, [s. l.], v. 5, n. 7, p. 1-9, 2015. DOI: <https://doi.org/10.1101/cshperspect.a021576> . Acesso em: 03 nov. 2023.

RIZZETTO, M *et al.* Immunofluorescence detection of new antigen-antibody system (delta/anti-delta) associated to hepatitis B virus in liver and in serum of HBsAg carriers. **Gut**, [s. l.], v. 18, n. 12, p. 997–1003, 1977. DOI: <https://doi.org/10.1136/gut.18.12.997> . Acesso em: 03 nov. 2023.

ROCCO, Caterina *et al.* Comparison of anti-hepatitis D virus (HDV) ETI-AB-DELTAK-2 assay and the novel LIAISON® XL MUREX anti-HDV assay in the diagnosis of HDV infection. **Diagnostic Microbiology and Infectious Disease**, [s. l.], v. 95, n. 4, p. 1-5, 2019. DOI: <https://doi.org/10.1016/j.diagmicrobio.2019.114873> . Acesso em: 03 nov. 2023.

ROULOT, D. *et al.* Origin, HDV genotype and persistent viremia determine outcome and treatment response in patients with chronic hepatitis delta. **Journal of Hepatology**, [s. l.], v. 73, n. 5, p. 1046–1062, 1 nov. 2020. DOI: <https://doi.org/10.1016/j.jhep.2020.06.038>. Acesso em: 13 dez. 2023

ROY, Supti *et al.* Spectroscopy goes viral: Diagnosis of hepatitis B and C virus infection from human sera using ATR-FTIR spectroscopy. **Clinical Spectroscopy**, [s. l.], v. 1, p. 1-14, 2019. DOI: <https://doi.org/10.1016/j.clispe.2020.100001>. Acesso em: 03 nov. 2023.

SCAGLIA, Elodie *et al.* Noninvasive assessment of hepatic fibrosis in patients with chronic hepatitis C using serum Fourier transform infrared spectroscopy. **Analytical and Bioanalytical Chemistry**, [s. l.], v. 401, n. 9, p. 2919–2925, 2011. DOI: <https://doi.org/10.1007/s00216-011-5402-8> . Acesso em: 03 nov. 2023.

SMITH, George. Filamentous Fusion Phage: Novel Expression Vectors That Display Cloned Antigens on the Virion Surface. **Science**, [s. l.], v. 228, n. 4705, p. 1315–1317, 1985. DOI: <https://doi.org/10.1126/science.4001944> . Acesso em: 03 nov. 2023.

SMITH, George P. Phage Display: Simple Evolution in a Petri Dish (Nobel Lecture). **Angewandte Chemie International Edition**, [s. l.], v. 58, n. 41, p. 14428–14437, 2019. DOI: <https://doi.org/10.1002/anie.201908308>. Acesso em: 03 nov. 2023.

STOCKDALE, Alexander J. *et al.* The global prevalence of hepatitis D virus infection: Systematic review and meta-analysis. **Journal of hepatology**, [s. l.], v. 73, n. 3, p. 523–532, 2020. DOI: <https://doi.org/10.1016/j.jhep.2020.04.008> . Acesso em: 03 nov. 2023.

SUREAU, Camille; NEGRO, Francesco. The hepatitis delta virus: Replication and pathogenesis. **Journal of Hepatology**, [s. l.], v. 64, n. 1, p. 102–116, 2016. DOI: <https://doi.org/10.1016/j.jhep.2016.02.013>. Acesso em: 03 nov. 2023.

TAN, Wen Siang; HO, Kok Lian. Phage display creates innovative applications to combat hepatitis B virus. **World Journal of Gastroenterology : WJG**, [s. l.], v. 20, n. 33, p. 11650–11670, 2014. DOI: <https://doi.org/10.3748/wjg.v20.i33.11650> . Acesso em: 03 nov. 2023.

TONELLI, Renata; COLLI, Walter; ALVES, Maria Júlia. Selection of binding targets in parasites using phage-display and aptamer libraries in vivo and in vitro. **Frontiers in Immunology**, [s. l.], v. 3, p. 1-16, 2013. DOI: <https://doi.org/10.3389/fimmu.2012.00419>. Acesso em: 03 nov. 2023.

TSELIGKA, Eirini D.; CLÉMENT, Sophie; NEGRO, Francesco. HDV Pathogenesis: Unravelling Ariadne's Thread. **Viruses**, [s. l.], v. 13, n. 5, p.1-22, 2021. DOI: <https://doi.org/10.3389/fimmu.2012.00419> . Acesso em: 03 nov. 2023.

TURON-LAGOT, Vincent *et al.* Targeting the Host for New Therapeutic Perspectives in Hepatitis D. **Journal of clinical medicine**, [s. l.], v. 9, n. 1, p. 1-16, 2020. DOI: <https://doi.org/10.3390/jcm9010222> . Acesso em: 03 nov. 2023.

USAI, C. *et al.* Review article: emerging insights into the immunopathology, clinical and therapeutic aspects of hepatitis delta virus. *Alimentary Pharmacology & Therapeutics*, v. 55, n. 8, p. 978–993, 16 mar. 2022. DOI: <http://doi.org/10.1111/apt.16807>. Acesso em: 13 dez 2023.

WANG, C *et al.* Development of a reverse transcription-loop-mediated isothermal amplification .pdf. **Letters in Applied Microbiology**, [s. l.], v. 56, n. 3, p.229-235, 2013. DOI: <https://doi.org/10.1111/lam.12039> . Acesso em: 03 nov. 2023.

WANG, K. S. *et al.* Structure, sequence and expression of the hepatitis delta (delta) viral genome. **Nature**, [s. l.], v. 323, n. 6088, p. 508–514, 1986. DOI: <https://doi.org/10.1038/323508a0> Acesso em: 03 nov. 2023.

WU, Dan *et al.* Phage Displayed Peptides to Avian H5N1 Virus Distinguished the Virus from Other Viruses. **PLOS ONE**, [s. l.], v. 6, n. 8, p. 1-6, 2011. DOI: <https://doi.org/10.1371/journal.pone.0023058> . Acesso em: 03 nov. 2023.

XU, Ling *et al.* Digital Droplet PCR for Detection and Quantitation of Hepatitis Delta Virus. **Clinical and translational gastroenterology**, United States, v. 13, n. 7, p. 1-11, 2022. DOI: <https://doi.org/10.14309/ctg.0000000000000509> . Acesso em: 03 nov. 2023.

XUE, Wenxiang *et al.* Identification and characterization of a novel nanobody against duck hepatitis A virus type 1. **Virology**, [s. l.], v. 528, p. 101–109, 2019. DOI: <https://doi.org/10.1016/j.virol.2018.12.013> . Acesso em: 03 nov. 2023.

YAN, Huan *et al.* Sodium taurocholate cotransporting polypeptide is a functional receptor for human hepatitis B and D virus. **eLife**, [s. l.], v. 1, p. 1-28, 2012. DOI: <https://doi.org/10.7554/eLife.00049> . Acesso em: 03 nov. 2023.

YU, Chung-Ming *et al.* A panel of anti-influenza virus nucleoprotein antibodies selected from phage-displayed synthetic antibody libraries with rapid diagnostic capability to distinguish diverse influenza virus subtypes. **Scientific Reports**, [s. l.], v. 10, n. 1, p.1-14, 2020. DOI: <https://doi.org/10.1038/s41598-020-70135-6> . Acesso em: 03 nov. 2023.